JGR Space Physics

RESEARCH ARTICLE
10.1029/2022JA030571

Special Section:
Fifteen Years of THEMIS Mission

On the Nature of Intense Sub-Relativistic Electron Precipitation

A. V. Artemyev[1], X.-J. Zhang[1], Y. Zou[2], D. Mourenas[3,4], V. Angelopoulos[1], D. Vainchtein[5], E. Tsai[1], and C. Wilkins[1]

[1]Department of Earth, Planetary, and Space Sciences, University of California, Los Angeles, CA, USA, [2]The University of Alabama in Huntsville, Huntsville, AL, USA, [3]CEA, DAM, DIF, Arpajon, France, [4]Laboratoire Matière en Conditions Extrêmes, Université Paris-Saclay, CEA, Arpajon, France, [5]Nyheim Plasma Institute, Drexel University, Camden, NJ, USA

Abstract Energetic electron precipitation into Earth's atmosphere is an important process for radiation belt dynamics and magnetosphere-ionosphere coupling. The most intense form of such precipitation is microbursts—short-lived bursts of precipitating fluxes detected on low-altitude spacecraft. Due to the wide energy range of microbursts (from sub-relativistic to relativistic energies) and their transient nature, they are thought to be predominantly associated with energetic electron scattering into the loss cone via cyclotron resonance with field-aligned intense whistler-mode chorus waves. In this study, we show that intense sub-relativistic microbursts may be generated via electron nonlinear Landau resonance with very oblique whistler-mode waves. We combine a theoretical model of nonlinear Landau resonance, equatorial observations of intense very oblique whistler-mode waves, and conjugate low-altitude observations of <200 keV electron precipitation. Based on model comparison with observed precipitation, we suggest that such sub-relativistic microbursts occur by plasma sheet ($0.1 - 10$ keV) electron trapping in nonlinear Landau resonance, resulting in acceleration to $\lesssim$200 keV energies and simultaneous transport into the loss cone. The proposed scenario of intense sub-relativistic ($\lesssim$200 keV) microbursts demonstrates the importance of very oblique whistler-mode waves for radiation belt dynamics.

Key Points:

- We report on intense sub-relativistic electron precipitation events observed by ELFIN CubeSats
- Sub-relativistic precipitation events are due to electron nonlinear Landau resonance with very oblique whistler waves
- Sub-relativistic precipitation events may indicate an enhancement of equatorial energetic electron fluxes

Correspondence to:
A. V. Artemyev,
aartemyev@igpp.ucla.edu

Citation:
Artemyev, A. V., Zhang, X.-J., Zou, Y., Mourenas, D., Angelopoulos, V., Vainchtein, D., et al. (2022). On the nature of intense sub-relativistic electron precipitation. *Journal of Geophysical Research: Space Physics*, *127*, e2022JA030571. https://doi.org/10.1029/2022JA030571

Received 19 APR 2022
Accepted 25 MAY 2022

1. Introduction

Energetic (several keV to several MeV) electron precipitation into the Earth's atmosphere is one of the most important mechanisms of electron loss from the outer radiation belt (see, e.g., reviews by Millan & Thorne, 2007; Shprits et al., 2008, and references therein). Besides the night-side curvature scattering (Artemyev, Orlova, et al., 2013; Capannolo et al., 2022; Sergeev & Tsyganenko, 1982; Yahnin et al., 1997), wave-particle resonant interaction is the main driver of such precipitation. Electrons of different energies interact resonantly with different wave modes, mainly: whistler-mode chorus waves (responsible for precipitation of sub-MeV electrons from the outer radiation belt, see, e.g., Horne and Thorne (1998); Horne and Thorne (2003); Ma, Li, Thorne, Nishimura, et al. (2016)), whistler-mode hiss waves (responsible for precipitation of sub-MeV electrons from the plasmasphere, see, e.g., Ma, Li, Thorne, Bortnik, et al. (2016); Mourenas et al. (2017)), and electromagnetic ion cyclotron (EMIC) waves (responsible for relativistic and ultra-relativistic electron precipitation from the outer radiation belts, see, e.g., Kersten et al. (2014); Blum, Halford, et al. (2015); Kubota et al. (2015); Grach and Demekhov (2020)). The most intense whistler-mode and EMIC waves interact with electrons nonlinearly (see reviews by Shklyar & Matsumoto, 2009; Albert et al., 2013; Artemyev, Neishtadt, Vainchtein, et al., 2018, and references therein) providing very intense and bursty precipitation events, called microbursts (Blum, Li, & Denton, 2015; Breneman et al., 2017; Capannolo et al., 2019; O'Brien et al., 2004; Shumko, Turner, et al., 2018; Zhang, Angelopoulos, et al., 2022). There exist many theoretical models of microbursts generated by whistler-mode waves (e.g., L. Chen et al., 2020; L. Chen et al., 2021) and EMIC waves (e.g., Kubota & Omura, 2017). Such models consider mostly field-aligned wave propagation, because the most intense waves observed are field-aligned chorus (Agapitov et al., 2013; Li, Santolik, et al., 2016; Santolík, Macúšová, et al., 2014) and EMIC (e.g., Min & Liu, 2016; Mithaiwala et al., 2013; Yu et al., 2016) waves.

Electron precipitation due to wave-particle resonant interactions corresponds to a decrease of the electron equatorial pitch-angle α_{eq} and a change of electron energy. Field-aligned chorus waves interact with electrons through the first cyclotron resonance. The nonlinear regime of this resonant interaction includes phase trapping (with α_{eq} and energy increase, see, e.g., Omura et al. (2015)) and phase bunching (with α_{eq} and energy decrease, see,

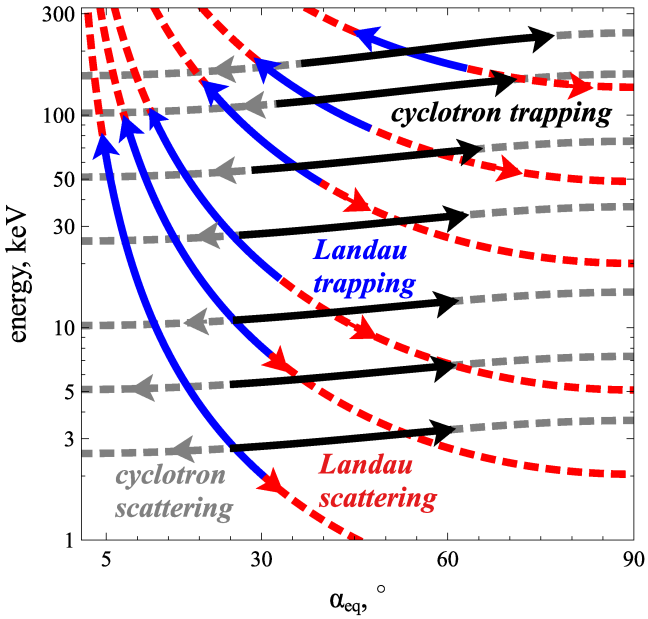

Figure 1. Resonance curves (Williams & Lyons, 1974) for cyclotron resonance with field-aligned whistler-mode wave and Landau resonance with very oblique whistler-mode wave. Resonance with monochromatic waves moves electrons along the shown curves. Thus, electron transport to the loss cone (toward smaller pitch-angles) almost does not change electron energy for cyclotron resonance, but significantly increases energy for Landau resonance. Nonlinear trapping direction is shown by solid lines, whereas nonlinear scattering (phase bunching) direction is shown by dashed lines. System parameters: L-shell is 6, wave frequency to equatorial cyclotron frequency is $f/f_{ce} = 0.35$, wave normal angle of very oblique whistler-mode wave is $\theta = \arccos(f/f_{ce}) - 5°$.

e.g., Albert (2000); Vainchtein et al. (2018)). The competition between phase trapping and phase bunching (Artemyev, Neishtadt, et al., 2016; Istomin et al., 1973; Shklyar, 2011; Solovev & Shkliar, 1986) controls the net electron transport into the loss cone, but all precipitating electrons lose energy, because precipitation is provided only by phase bunching. Thus, both linear and non-linear electron interaction with chorus via the cyclotron resonance is associated with electron deceleration. Thus, not only is net energy lost from the magnetosphere due to precipitation, but this energy is lost by equatorial electrons of equal or higher energy, resulting in a decay of the radiation belt (energetic electron) flux. Precipitation due to electron resonance with EMIC waves is due to phase trapping, which moves electrons into the loss cone (Albert & Bortnik, 2009; Grach & Demekhov, 2020; Grach et al., 2021; Kubota & Omura, 2017). Such trapping, just like electron resonance with EMIC waves in general (Ni et al., 2015; Summers & Thorne, 2003), does not change the electron energy, that is, EMIC driven precipitation events are associated with energetic electron flux decrease simply due to atmospheric loss without deceleration of equatorial electrons. As microbursts are very intense (associated with orders of magnitude increases of precipitating flux at low-altitude spacecraft measurements), this precipitation pattern is often considered as one of the main mechanisms of energetic electron loss (e.g., Thorne et al., 2005).

The energy range of microburst precipitation is quite wide (e.g., Zhang, Angelopoulos, et al., 2022): there are both relativistic microbursts (Blum, Li, & Denton, 2015; O'Brien et al., 2004), microbursts of few hundreds of keV (Capannolo et al., 2019; Shumko, Sample, et al., 2018), and even of tens of keV (Blake & O'Brien, 2016). Moreover, recent investigations show strong correlations between relativistic microbursts and tens of keV electron precipitation responsible for diffuse aurora (Y. Miyoshi et al., 2020; K. Miyoshi Y. et al., 2021; Shumko et al., 2021). Although relativistic microbursts may be generated by electron resonances with EMIC waves (Blum, Halford, et al., 2015; Grach & Demekhov, 2020; Kubota et al., 2015), sub-relativistic electrons can rarely interact resonantly with EMIC waves (e.g., L. Chen et al., 2019) and hence they are often attributed to electron scattering by chorus waves (Breneman et al., 2017; Mozer et al., 2018; Y. Miyoshi et al., 2020).

Although field-aligned chorus waves are the most intense whistler-mode wave population in the radiation belt (Agapitov et al., 2013; Li et al., 2011), this is not the sole wave population present in this region. There is also a significant population of very oblique whistler-mode waves (almost electrostatic mode, see Artemyev, Agapitov, et al. (2016)) propagating near the resonance cone angle (Agapitov et al., 2013; Agapitov et al., 2018; Li, Santolik, et al., 2016). These oblique waves can interact resonantly with electrons through Landau resonance (e.g., Nunn & Omura, 2015; Shklyar & Matsumoto, 2009) and can accelerate electrons efficiently via phase trapping (Agapitov et al., 2014; Artemyev, Krasnoselskikh, et al., 2012; Hsieh et al., 2020; Hsieh & Omura, 2017a). The corresponding Landau resonant energies are much lower than cyclotron resonant energies with quasi-parallel waves, allowing very oblique waves to resonate with 100 eV - 10 keV electrons (Artemyev, Agapitov, et al., 2015, 2016; Mourenas et al., 2014) which can almost never be scattered by field-aligned lower-band chorus waves (Li et al., 2010). Moreover, in contrast to the cyclotron resonance associated with an energy decrease of precipitating electrons, the Landau resonant trapping is associated with energy increase (see Figure 1 for resonance curves and directions of electron motion in energy, pitch-angle space due to cyclotron and Landau resonances). In other words, precipitating electrons (those with decreasing α_{eq}) are simultaneously accelerated, corresponding to an increase of low-α_{eq} energetic electron flux (Agapitov et al., 2015b). Since very oblique whistler-mode waves can be quite intense (Agapitov et al., 2014; Cattell et al., 2008; Cully, Bonnell, & Ergun, 2008; Wilson et al., 2011), these waves may in principle interact nonlinearly with electrons and efficiently trap them through Landau resonance (Agapitov et al., 2015b; Mourenas et al., 2016). But can such trapping result in intense (microburst-like) electron precipitation?

This study aims to address this question by combining a theoretical investigation of electron phase trapping into Landau resonance, using observed wave characteristics, and low-altitude observations of electron precipitation. We show that the phase trapping into Landau resonance (Landau-trapping) can indeed create an intense electron flux peaking within the loss cone. However, in contrast to precipitation due to cyclotron resonance, precipitation due to Landau-trapping does not correspond to energetic electron flux decay. Instead, Landau-trapping precipitation is accompanied by significant electron acceleration and the formation of an additional sub-relativistic (up to ≤200 keV) electron population in the outer radiation belt.

The paper consists of four sections. In Section 2, we analyze an event with Time History of Events and Macroscale Interactions during Substorms (THEMIS) spacecraft (Angelopoulos, 2008) equatorial measurements of very oblique whistler-mode waves, together with conjugate low-altitude ELFIN CubeSat (Angelopoulos et al., 2020) measurements of electron precipitation. We supplement the analysis of this event by Defense Meteorological Satellite Program (DMSP) satellite measurements of <10 keV electron precipitation (Hardy et al., 1984; Rich et al., 1985), because electrons of such energies can only interact with whistler-mode lower-band chorus waves through Landau resonance. In Section 3, we describe the theoretical model of electron acceleration and precipitation by Landau-trapping. This model is based on the mapping technique for the evaluation of electron flux dynamics due to nonlinear interactions with whistler-mode waves (Artemyev et al., 2020b; Artemyev, Neishtadt, Vasiliev, Zhang, et al., 2021). We generalize the mapping technique for systems with a realistic distribution of waves (in terms of as frequency and time-series envelope amplitude), and apply it to the data set obtained from THEMIS around the equatorial plane. Our mapping simulation results of electron flux expected at ionospheric altitude are compared with ELFIN observations of electron precipitation events. In Section 4, we discuss the results of this comparison and speculate about the importance of Landau resonance with very oblique whistler-mode waves for intense sub-relativistic electron precipitation.

2. THEMIS, ELFIN, and DMSP Observations on 2021-01-01

We first analyze a precipitation event with conjugate THEMIS and ELFIN observations on the dayside in the inner magnetosphere. Figure 2 is an overview of THEMIS E measurements on 2021-01-01 from 22:20 to 23:30 UT in the dayside inner magnetosphere, when the spacecraft moved outward from $L \sim 7$ to $L \sim 9$ (L is evaluated with the Tsyganenko (1989) magnetic field model). Fluxgate magnetometer data with 1/4s resolution (Auster et al., 2008) shows that THEMIS E was around the equator with GSM $B_z \gg |B_x|, |B_y|$ (see panel (a)). THEMIS search coil (Le Contel et al., 2008) and electric field instrument (Bonnell et al., 2008) measurements are used to check the wave activity. Panels (b) and (c) show magnetic and electric field spectra obtained from these instruments (32 frequency channels in $10 - 4000$ Hz range) in the *fff* data set (see Cully, Ergun, et al., 2008). There is strong whistler-mode wave activity within the frequency range $f/f_{ce} \in [0.2, 0.4]$, where the electron cyclotron frequency f_{ce} is calculated from in-situ measurements from the fluxgate magnetometer. Using plasma density estimates from the spacecraft potential (Nishimura et al., 2013), we plot the plasma frequency to electron gyrofrequency ratio, f_{pe}/f_{ce}, in panel (d). This ratio is quite low ($f_{pe}/f_{ce} \sim 3$) for $L \in [6, 8]$, suggesting atypical conditions of whistler-mode wave generation and wave resonant interaction with electrons.

Figure 3 shows several whistler-mode wave packets. We use electric field measurements in the field-aligned coordinate system, because 3D wave magnetic field measurements are not yet fully calibrated in the whistler-mode range during this interval. All wave packets show a large parallel electric field component, suggesting the presence of very oblique whistler-mode waves (Artemyev, Agapitov, et al., 2016). Using f_{pe}/f_{ce} from Figures 2d and 3d electric fields from Figure 3, we estimate the wave normal angle θ (angle between wave-vector and the background magnetic field) for the displayed wave-packets: $\theta \in [60, 70]$ (see details of θ estimation method in Ni, Thorne, Meredith, Shprits, and Horne (2011); Agapitov et al. (2014)), with a Gendrin angle $\theta_g = \text{acos}(2f/f_{ce}) \approx 45°$ and a resonance cone angle $\theta_r = \text{acos}(f/f_{ce}) \approx 69°$. Thus, the observed waves indeed propagate obliquely with $\theta \in [\theta_g, \theta_r]$, that is, in the quasi-electrostatic mode (see statistics of such whistler-mode waves in Agapitov et al. (2013); Li, Santolik, et al. (2016)), and can interact with electrons through the Landau resonance (Artemyev, Agapitov, et al., 2016; Shklyar & Matsumoto, 2009).

The generation, and propagation without significant damping, of very oblique whistler-mode waves requires a very specific type of electron distribution function (Artemyev & Mourenas, 2020; Ma et al., 2017; Mourenas et al., 2015). For the observed waves, the Landau resonant energy at the equator starts at $m_e(\omega/k_\parallel)^2/2 \sim 1 - 5$keV,

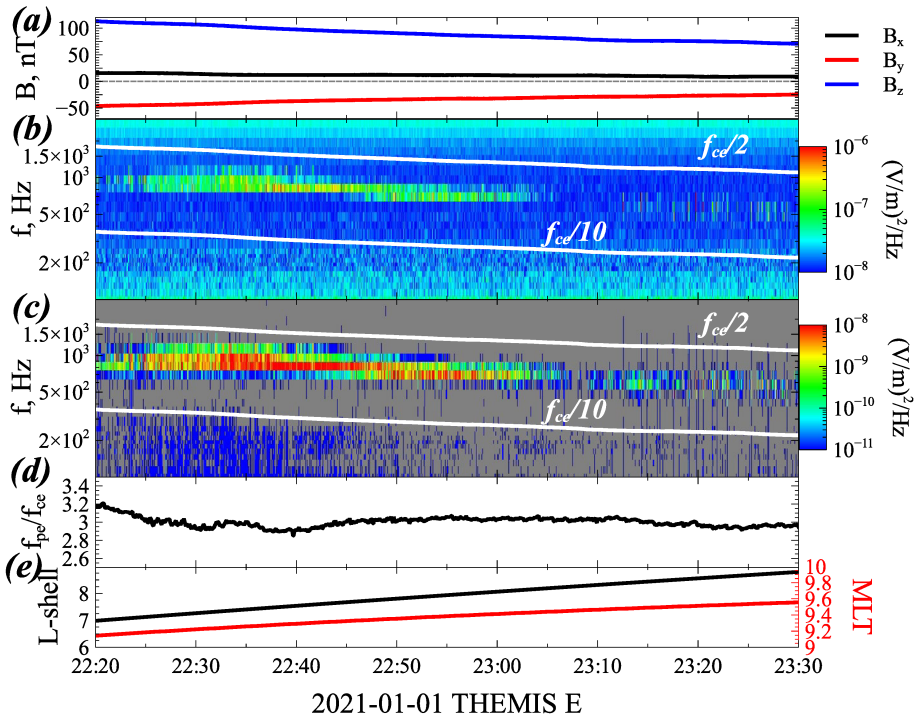

Figure 2. An overview of THEMIS E observations on 2021-01-01: (a) GSM magnetic fields, (b) and (c) magnetic and electric field spectra (for data format see Cully, Ergun, et al., 2008) with fractions of f_{ce} shown by horizontal curves, (d) plasma frequency to gyrofrequency ratio.

where $\omega = 2\pi f$ is determined by measurements of wave spectrum and $k_{||}$ is determined by the wave dispersion for a measured wave normal angle. For typical electron distributions with a smoothly decreasing density toward higher parallel electron energy, Landau damping by these dense suprathermal electrons would quickly reduce the wave intensity to the noise level (Kennel, 1966; Bortnik et al., 2007; L. Chen et al., 2013). Accordingly, such very oblique waves are mainly associated with electron distributions having a plateau or weak field-aligned beams around the Landau resonant energy at the equator (Li, Mourenas, et al., 2016; R. Chen et al., 2019; Artemyev & Mourenas, 2020; Kong et al., 2021). Figure 4c shows that THEMIS E measured such a plateau both in the field-aligned and transverse phase space densities during the entire interval of whistler-mode wave observations (note also a weak field-aligned anisotropy of ~1–5 keV electrons in Figure 4b). The omnidirectional plateau represents the addition of a ring/shell electron distribution (see Figure 4a) with an almost null gradient in parallel velocity, that is, the absence of an intense negative distribution function gradient in parallel velocity that would provide Landau damping. Therefore, the conditions during this event (low f_{pe}/f_{ce} and absence of Landau damping) are favorable for very oblique wave generation and amplification (Artemyev, Agapitov, et al., 2016; Mourenas et al., 2015).

An interesting and important feature of the observed whistler-mode wave activity is the transient nature of wave bursts (see Figure 2b), which may be due to quasi-periodic wave generation modulated by compressional ultra-low-frequency waves (Li et al., 2011; Li, Thorne, et al., 2011; Xia et al., 2016; Zhang, Chen, et al., 2019). Such compressional waves were indeed observed concurrently by THEMIS E (not shown) over a wide frequency range. As the generation of very-oblique whistler-mode waves is associated with the Landau resonant scattering of <10 keV electrons around the equator (Agapitov et al., 2016; Artemyev, Agapitov, et al., 2016; Li, Mourenas, et al., 2016), we may expect quasi-periodic enhancements of electron precipitating fluxes. To check this hypothesis, we examine measurements of precipitating electrons by the Precipitating Electron and Ion Spectrometer onboard two DMSP satellites (Hardy et al., 1984; Rich et al., 1985). Figure 5 (right column) shows DMSP electron spectra around the interval of THEMIS E observations of very oblique whistler-mode waves. There are clear spatially/temporally localized enhancements of ~5 keV electron precipitation seen by DMSP at $6 < L < 11$. Such precipitation enhancements were not seen before the interval of THEMIS observations of oblique whistler-mode waves (see DMSP electron spectra in Figure 5 (left column)). Therefore, DMSP spectrometer measurements of

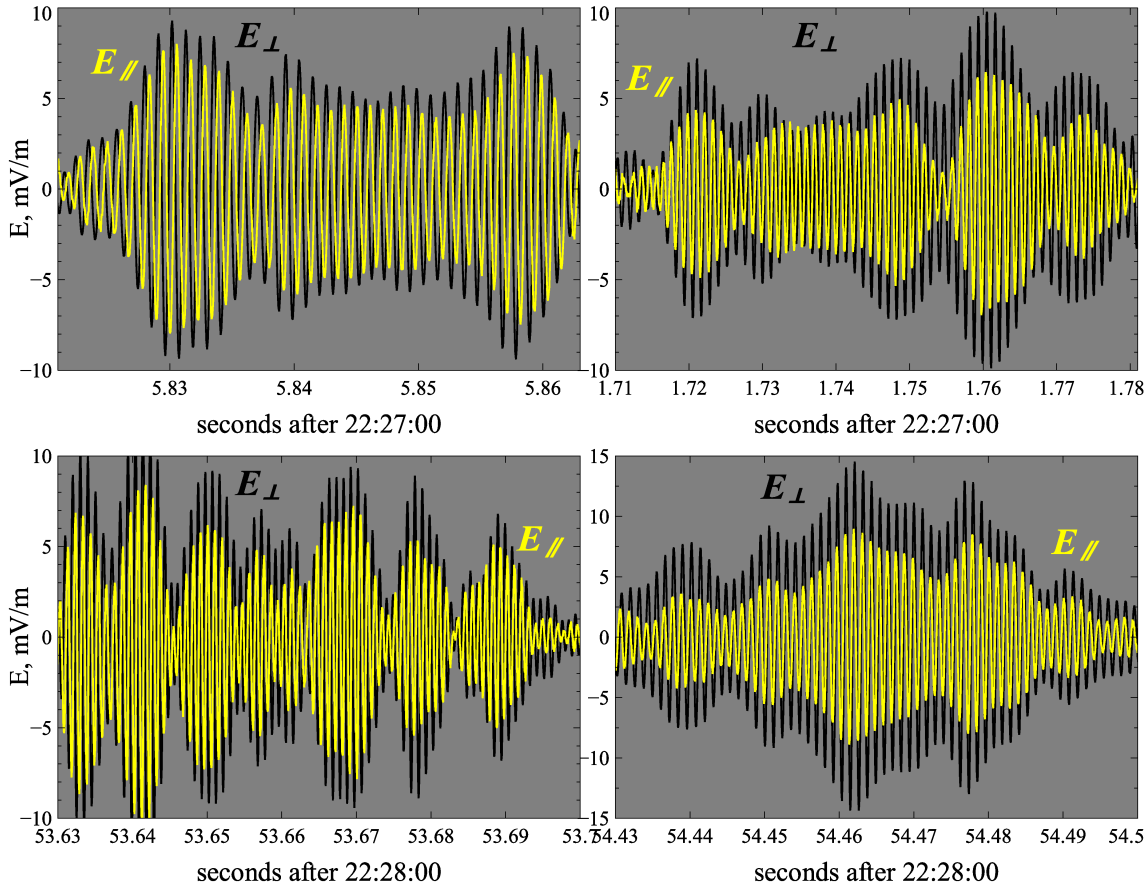

Figure 3. Four examples of whistler-mode wave packets during the event in Figure 2.

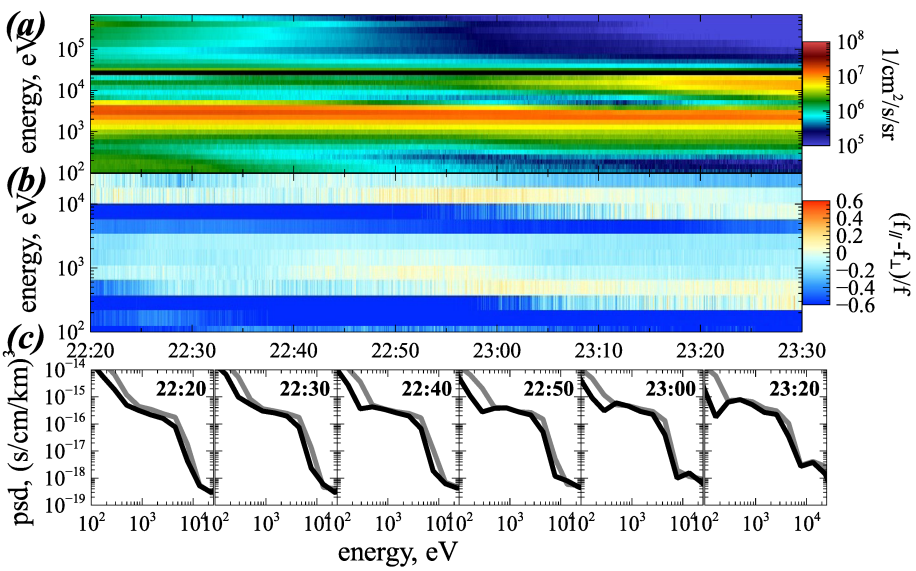

Figure 4. Electron flux measurements by THEMIS E during the event in Figure 2: (a) omnidirectional energy fluxes, (b) flux anisotropy in the <30 keV range, (c) parallel (black) and transverse (gray) phase space densities at several times.

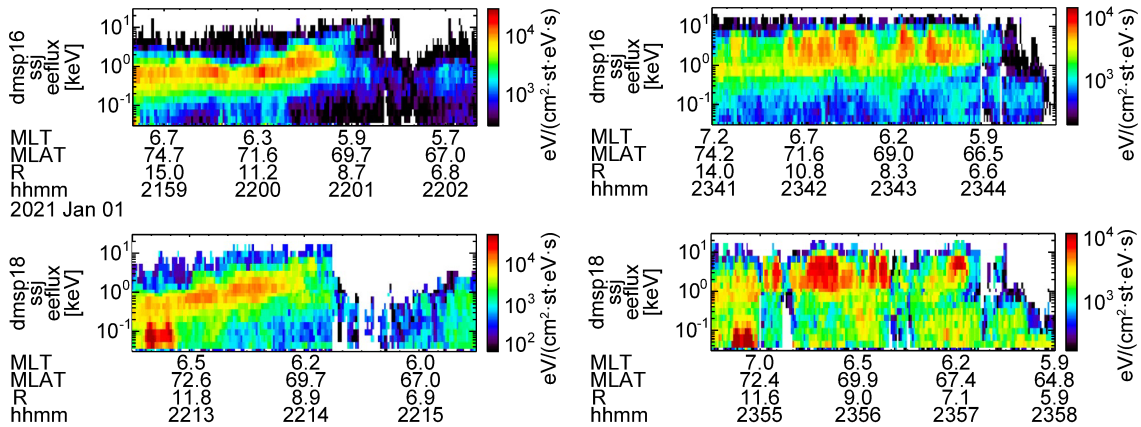

Figure 5. Precipitating electron spectra from four Defense Meteorological Satellite Program (DMSP) orbits (two orbits of DMSP 16 and two orbits of DMSP 18) covering the interval of THEMIS and ELFIN observations: left column panels show DMSP data obtained before the detection of quasi-periodic oblique whistler-mode waves on THEMIS, whereas the right column panels show DMSP data during THEMIS observations of quasi-periodic oblique whistler-mode waves. Satellite MLT, magnetic latitude (MLT), *L*-shell (*R*) are shown below each panel.

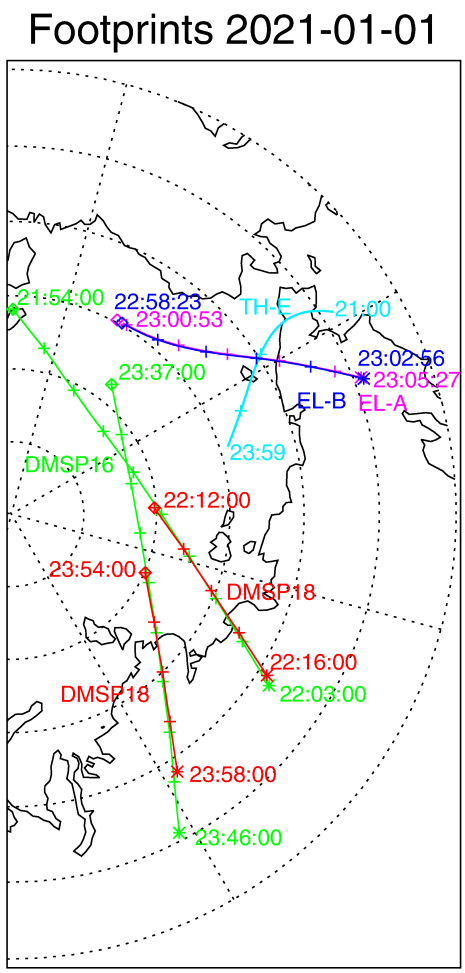

Figure 6. Footprints of THEMIS E, Defense Meteorological Satellite Program 16 and 18, and ELFIN A and B orbits for the event from Figures 2 and 5.

<10 keV electron precipitation are consistent with the presence of a transient (quasi-periodic) equatorial generation of very oblique whistler-mode waves.

Let us now consider conjugate low-altitude ELFIN observations and equatorial THEMIS E measurements of very oblique whistler-mode waves. There are a couple of orbits of ELFIN A and B within the same time interval and *L*-shell, MLT range (see Figure 6 for THEMIS, DMSP, and ELFIN orbits as a function of MLT and *L*-shell). Figures 7a and 7b shows that the energy spectra of trapped electron fluxes on both ELFIN CubeSats demonstrate a typical outer radiation belt structure, as indicated by the flux (and energy range) increase from $L \sim 11$ to $L \sim 5$ (where the plasmapause was at the time, according to the THEMIS E plasma data), and the disappearance of <500 keV fluxes due to effective scattering at these energies by plasmaspheric hiss waves (Ma, Li, Thorne, Bortnik, et al., 2016; Mourenas et al., 2017; Mourenas & Ripoll, 2012). Within the *L*-shell range corresponding to the outer radiation belt, ELFIN observed transient, strong precipitation of <200 keV electrons (see panels (c,d)). The timescale of these precipitation bursts is about (or even less than) ELFIN's half-spin-period, 1.5s. Both ELFIN CubeSats show similar patterns of transient precipitation, but the temporal (spatial) distributions of precipitation bursts are different on these two spacecraft moving along the same orbit with an ~2 min time delay. Therefore, we infer that these precipitation events are probably driven by electron scattering by transient whistler-mode waves which, due to their amplitude modulation by ULF waves, do not maintain the same spatial distribution at the equator over time intervals longer than ~1–2 min.

Figures 7e and 7f shows the ratio of precipitating to trapped electron fluxes. Most of the precipitation bursts reach a ratio ~1 at energies <200 keV, that is, they represent very strong precipitation with an entirely filled loss cone, roughly corresponding to the so-called strong diffusion limit (Kennel, 1969). Note that ELFIN is a spinning CubeSat (Angelopoulos et al., 2020) and that different pitch-angles are measured at slightly different times within the 1.5s half-spin-period. Thus, sub-second precipitation events may demonstrate precipitating fluxes even higher than trapped fluxes, but this can either be an effect of a specific precipitation mechanism (see Zhang, Artemyev, et al., 2022) or it can be an artifact due to aliasing, that is, the absence of

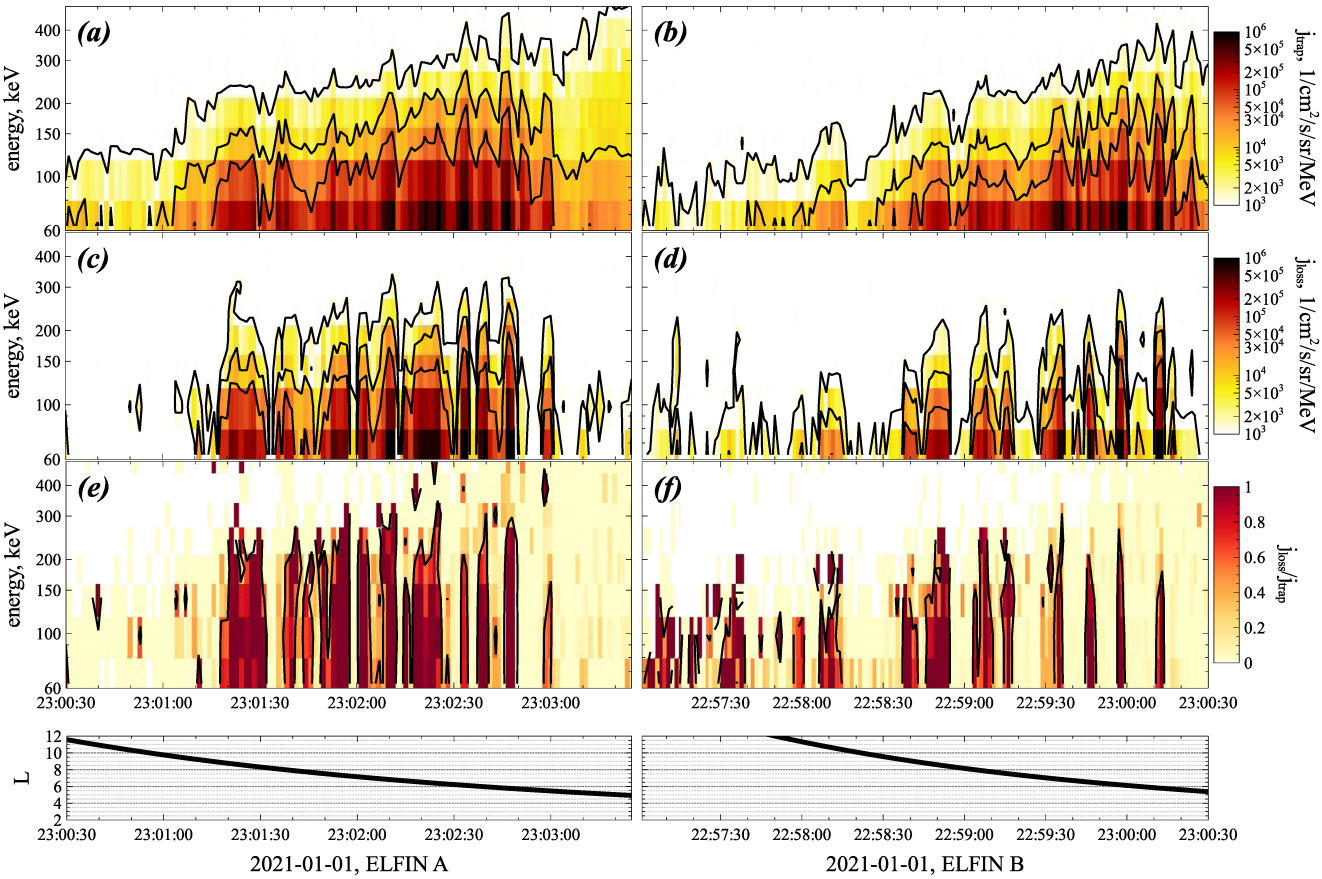

Figure 7. An overview of ELFIN A and B measurements for the event from Figure 2: (a, b) trapped fluxes, (c, d) precipitating fluxes, (e, f) precipitating to trapped flux ratio. Bottom panels shows ELFIN *L*-shells from (Tsyganenko, 1989) model.

strictly simultaneous measurements of trapped and precipitating fluxes. Nevertheless, the observed precipitation events are transient, short-scale, and very intense, as expected for microbursts.

3. Theory of Nonlinear Landau Resonance

In contrast to classical models of microburst precipitation events due to cyclotron resonance with field-aligned chorus waves (e.g., L. Chen et al., 2020; L. Chen et al., 2022), precipitation events in Figure 7 are observed in conjunction with equatorial measurements of very oblique whistler-mode waves (see Figure 5). Therefore, an alternative mechanism of precipitation due to the Landau resonance should be invoked here (see Figure 1 and Agapitov et al. [2015b]). To verify the efficiency of precipitation due to Landau resonance, we use the mapping technique proposed in Artemyev et al. (2020b). This technique provides an alternative to test particle simulations (widely used for investigation of nonlinear resonances, see, e.g., Tao et al. [2013]; Gan et al. [2020]; Agapitov et al. [2015b]; Allanson et al. [2020]; Zhang, Agapitov, et al. [2020]), to the Green function method (see, e.g., Omura et al. [2015]; Hsieh and Omura [2017b]), or to the inclusion of integral operators into the Fokker-Plank equation (see, e.g., Artemyev, Neishtadt, Vasiliev, and Mourenas [2018]; Vainchtein et al. [2018]). The advantages of the mapping technique are that (a) it combines the analytical theory for energy/pitch-angle change in nonlinear resonance (Neishtadt, 1975, 1999), (b) it allows to incorporate the effects of resonant interactions with a wave ensemble sharing the properties of the observed waves (Artemyev, Neishtadt, Vasiliev, Zhang, et al., 2021; Vainchtein et al., 2018; Zhang, Artemyev, et al., 2022), and (c) it is computationally fast. This technique resembles the method of stochastic differential equations for the Fokker-Plank equation (e.g., Tao et al., 2008), but it further includes nonlinear resonance effects such as phase trapping and bunching (Artemyev et al., 2020b).

The mapping technique applicability is based on a set of assumptions:

1. Although the wave ensemble (collected over a long time interval) can have a quite broad distribution over wave parameters (amplitudes, frequencies, etc.), the waves are assumed to be sufficiently spread along magnetic field lines so that there can be no resonance overlapping, that is, it is assumed that there is no destruction of nonlinear wave-particle interaction due to resonance overlap (Nunn, 1986; Tao et al., 2013). This condition is generally satisfied for narrow-band intense whistler-mode waves, but it can be violated by various secondary effects in the presence of non-resonant noise (Artemyev, Mourenas, et al., 2015; Brinca, 1972), wave phase decoherence (Zhang, Agapitov, et al., 2020), or wave-packet modulation (An et al., 2022; Gan et al., 2020; Gan et al., 2022; Hiraga & Omura, 2020; Nunn et al., 2021; Zhang, Mourenas, et al., 2020). The inclusion of such effects, which limit the efficiency of nonlinear resonant interaction, is generally possible (e.g., Artemyev, Neishtadt, Vasiliev, & Mourenas, 2021; Mourenas et al., 2018), but since it requires significant modifications to theoretical estimates, we did not include these effects into the current version of the mapping technique.
2. Each of the wave-particle resonant interactions should be considered independently, that is, we assume no correlation of electron gyrophase between two successive resonant interactions. Such correlations may significantly modify the efficiency of electron scattering by waves (see discussion in, e.g., Allanson et al., 2022; Osmane & Lejosne, 2021), but for realistic, inhomogeneous magnetic fields and realistic whistler-mode wave amplitudes, effects due to phase correlations are negligibly weak (see discussions in Artemyev et al., 2020b; Artemyev et al., 2020a).
3. The nonlinear resonant wave-particle interaction cannot transport electrons outside the (energy, pitch-angle) domain where such an interaction is possible, that is, there is no lost phase trapping/phase bunching along the electron orbit. This condition is satisfied owing to the asymptotes of (energy, pitch-angle) changes around the boundaries of the domain of nonlinear resonant interactions (see Artemyev et al. [2019] and Appendix B in Artemyev, Neishtadt, Vasiliev, Zhang, et al. [2021]).

The mapping technique describes electron energy γ (electron gamma factor) and equatorial pitch-angle α_{eq} changes due to resonant interactions (note that these variables remain constant between resonant interactions) as

$$\gamma_{n+1} = \gamma_n + \begin{cases} \Delta\gamma_{trap}, & \xi \in [0,\pi] \\ \Delta\gamma_{scat}, & \xi \in (\pi,1] \end{cases}, \qquad \alpha_{eq,n+1} = \alpha_{eq,_n} + \begin{cases} \Delta\alpha_{eq,trap}, & \xi \in [0,\pi] \\ \Delta\alpha_{eq,scat}, & \xi \in (\pi,1] \end{cases} \tag{1}$$

where n is the number of resonant interactions (the mapping iteration number), $\Delta\gamma_{trap}$ and $\Delta\gamma_{scat}$ are energy changes due to trapping and bunching (the same for α_{eq}), $\pi \leq 1$ is the trapping probability (π can be interpreted as the relative number of resonant electrons which experienced trapping during a single resonant interaction), and ξ is a random value with a uniform distribution over [0, 1] (Artemyev et al., 2020b). Three main characteristics of the nonlinear resonant interactions, $\Delta\gamma_{trap}$, $\Delta\gamma_{scat}$, and π (note that $\Delta\alpha_{eq,trap}$, $\Delta\alpha_{eq,scat}$ can be recalculated from $\Delta\gamma_{trap}$, $\Delta\gamma_{scat}$) depend on electron energy γ_n and equatorial pitch-angle $\alpha_{eq,n}$, and on wave and background plasma characteristics. The energy change due to the phase bunching (also called nonlinear scattering) is the mean energy change of all electrons that did not experience trapping within a single resonant interaction. This is a local characteristic depending on particle, wave, and background magnetic field characteristics of the resonance location (or the latitude of resonance). Examples of $\Delta\gamma_{scat}$ evaluation for various systems with nonlinear resonance can be found in (Albert, 2002; Artemyev, Vasiliev, Mourenas, Agapitov, & Krasnoselskikh, 2014; Artemyev, Vasiliev, Mourenas, Agapitov, Krasnoselskikh, et al., 2014; Itin et al., 2000; Neishtadt et al., 2011; Shklyar, 2011), whereas the basic theory of $\Delta\gamma_{scat}$ evaluation can be found in (Albert, 1993; Karpman et al., 1974; Karpman & Shkliar, 1977; Neishtadt, 1999). There is an important relation between $\Delta\gamma_{scat}$ and the trapping probability: $\pi = \nabla\Delta\gamma_{scat}$ (see Artemyev, Neishtadt, et al., 2016; Artemyev, Neishtadt, Vainchtein, et al., 2018), where the gradient is along the resonance curve $n_r\gamma - (\omega/\Omega_{ce,eq})(\gamma^2 - 1)\sin^2\alpha_{eq}/2 = const$ (Shklyar & Matsumoto, 2009) that connects γ and α_{eq} changes for a given wave frequency ω, equatorial electron cyclotron frequency $\Omega_{ce,eq}$, and resonant number n_r ($n_r = 1$ for the first cyclotron resonance and $n_r = 0$ for the Landau resonance). Examples of the theoretical evaluation and numerical verification of π for electron resonant interaction with whistler-mode waves can be found in Artemyev, Vasiliev, Mourenas, Agapitov, and Krasnoselskikh (2014); Artemyev, Vasiliev, et al. (2015); Artemyev et al. (2020b). In contrast to $\Delta\gamma_{scat}$ and π, the energy change due to trapping $\Delta\gamma_{trap}$ is a nonlocal characteristic and depends on the wavefield distribution along magnetic field lines (see, e.g., Artemyev, Krasnoselskikh, et al., 2012; Agapitov et al., 2014; Artemyev, Neishtadt, Vasiliev, & Mourenas, 2018), $B_w(\lambda)$ where λ is the magnetic latitude. Such a distribution can be derived from empirical models of whistler-mode wave

intensity (Agapitov et al., 2015a, 2018; Wang & Shprits, 2019) or from numerical tracing of whistler-mode waves (Hsieh & Omura, 2017b; Omura et al., 2015). For very oblique waves, we use a simplified model that fits the observed $B_w(\lambda)$ distribution obtained from satellite statistics by Agapitov et al. (2018):

$$B_w = B_{w,eq} \cdot \frac{1}{2}\left(1 + \tanh\left(\lambda/\delta\lambda_1\right)\right) \cdot \exp\left(-\lambda^2/\delta\lambda_2^2\right) \tag{2}$$

where $\delta\lambda_1$ determines the spatial extent of the wave generation region, and $\delta\lambda_2$ determines the latitude range of wave propagation before damping at middle latitudes. This model describes waves in the $\lambda > 0$ hemisphere, and we assume a symmetric wavefield distribution relative to the equator, that is, $B_w(\lambda) = B_w(-\lambda)$. Wave frequency can be assumed to be fixed along the wave propagation (or slowly varying in time, if we deal with chorus waves), whereas the wave number profile $k(\lambda)$ can be obtained from the cold plasma dispersion (Stix, 1962) for a given wave normal angle distribution $\theta(\lambda)$ at this particular frequency. For very oblique whistler-mode waves, we use a $\theta = \theta_r(\lambda) - \Delta\theta$ model, with $\theta_r = \arccos(\omega/\Omega_{ce})$ being the resonant cone angle and $\Delta\theta = const$ the model parameter specifying the wave normal angle deviation from θ_r. This wave normal angle model is based on previous observations of very oblique whistler-mode wave propagation around the resonance cone angle (Agapitov et al., 2013; Li, Santolik, et al., 2016). The cold plasma dispersion relation does not work for $\Delta\theta \to 0$, where the thermal electron contribution to the wave dispersion properties becomes crucial (Sazhin & Horne, 1990). Theoretical estimates (Artemyev, Agapitov, et al., 2016; Mourenas et al., 2014) and spacecraft observations (Ma et al., 2017) suggest that the minimum $\Delta\theta$ can be determined from the limitation of the wave refractive index $N = kc/\omega$ to values $N < N_{hot} \approx 100$–300 for typical thermal electron energies in the inner magnetosphere.

During Landau resonance $\left(\omega\gamma - k_\parallel c\sqrt{\gamma^2 - 1}\cos\alpha = 0\right)$, the electron propagates in the same direction as the wave, in contrast to cyclotron resonance characterized by opposite propagations of wave and electron. For a fixed wave frequency at Landau resonance, the resonance curve $(\omega/\Omega_{ce,eq})(\gamma^2 - 1)\sin^2\alpha_{eq}/2 = const$ (Shklyar & Matsumoto, 2009) is given by the equation of the constant magnetic moment (we use the normalized moment $I_x = (\omega/\Omega_{ce,eq})(\gamma^2 - 1)\sin^2\alpha_{eq}/2$). Combining this equation with the resonance condition, we obtain the equation for dependence of the Landau resonant energy on the magnetic latitude:

$$\gamma_R = \frac{1}{\sqrt{1 - (\omega/ck_\parallel)^2}}\sqrt{1 + 2I_x\Omega_{ce}} \tag{3}$$

Figure 8a shows the latitude of resonance $\lambda_R(\gamma, \alpha_{eq})$, whereas Figure 8b shows $\lambda_R(\gamma_R)$ for fixed I_x. Small pitch-angle ($\alpha_{eq} < 30°$) low-energy (<10 keV) electrons may resonate with waves around the equatorial plane ($\lambda_R < 15°$), whereas energetic (~150 keV) electrons reach resonance only at $\lambda_R > 30°$. The wave intensity increases with latitudes $dB_w/d\lambda > 0$ around the equator (Agapitov et al., 2018; Omura et al., 2008). This condition suggests that electrons may be trapped by waves. Being trapped at small λ_R, electrons are transported by the wave to higher latitudes (with a decrease of their pitch-angle) and escape from the resonance at a latitude where $dB_0/d\lambda$ becomes sufficiently strong (for a precise description of the trapping and de-trapping conditions, see, e.g., Artemyev, Krasnoselskikh, et al. (2012); Artemyev, Vasiliev, et al. (2013)). Such an electron transport is associated with an energy increase, for example, a 5 keV equatorial electron can gain 100 keV before reaching $\lambda_R \sim 30°$ and finishing within the loss cone (see Figure 8b). Therefore, the trapping moves lower energy/larger pitch-angle electrons toward the larger energy/lower pitch-angle region in phase space (see schematic in Figure 1). The Landau resonance scattering moves electrons along the same resonance curve $I_x = const$, but in the direction opposite to the trapping motion. Therefore, Landau resonance results in electron drifts toward smaller energy/larger pitch-angle (the phase bunching effect) and more rare jumps to larger energy/smaller pitch-angle (the phase trapping effect). Figure 8c shows three examples of such electron dynamics evaluated with the mapping technique (1) for typical wave characteristics.

3.1. Mapping Model for Observed Wave Characteristics

Near-equatorial spacecraft measurements of whistler-mode waves provide distributions of wave characteristics, for example, the average wave intensity for various frequency ranges, L-shells, MLT, and λ (Meredith et al., 2001, 2012; Agapitov et al., 2013, 2015a). Such time-averaged intensities can be directly applied to the evaluation of quasi-linear diffusion rates (e.g., Agapitov et al., 2018; Horne et al., 2013; Ma et al., 2018), but

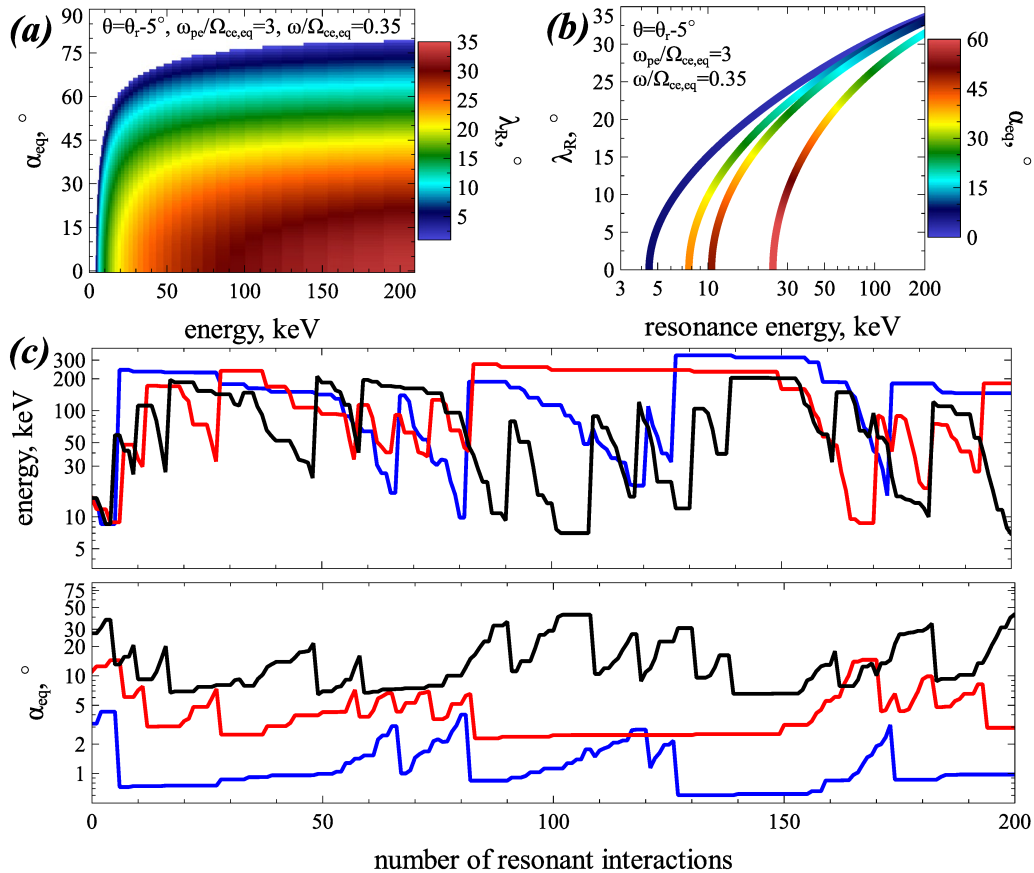

Figure 8. Panel (a) shows the resonance latitudes as a function of energy and equatorial pitch-angle. Panel (b) shows variations of the trapped particle latitude with energy given by Equation 3, that is, each curve shows the resonant condition for constant I_x. Colors denote variations of the equatorial pitch-angle. Panels (c) shows energy and equatorial pitch-angle for three trajectories evaluated with the mapping technique (1).

they are not suitable for the evaluation of nonlinear wave-particle interactions. Instead of time-averaged intensities, the nonlinear resonance models require distributions (occurrence rates) of intense waves that can interact with electrons nonlinearly (Zhang et al., 2018; Zhang, Mourenas, et al., 2019). Therefore, we use THEMIS E measurements during the event in Figure 2 to obtain the distribution of wave amplitudes E_w, as inferred from the wave frequency spectrum $\mathcal{E}_w^2(f)$: $E_w^2 = \int_{f_{ce}/20}^{f_{ce}/2} \mathcal{E}_w^2(f)df$. As shown in Figure 9a, most waves have amplitudes <3 mV/m. However, E_w here is inferred from the 1s-averaged spectrum (Cully, Ergun, et al., 2008) and the actual magnitude of individual wave-packets is often significantly larger (see Figure 3). To account for such an underestimation of E_w due to time averaging, we introduce a multiplicative factor K, that is, we assume that electrons interact with waves of amplitudes $K \times E_w$. To keep the same average intensity as without the K factor, we assume that electrons resonate with waves only a fraction $(1/K^2)$ of the simulation time, whereas during the remaining fraction $(1 - 1/K^2)$ of the time there is no resonant interaction.

The wave-particle resonant interaction is not determined solely by E_w, but also by the wave frequency, wave normal angle, and the $E_w(\lambda)$ profile along the magnetic field line. The wave frequency can be determined from the wave frequency spectrum: $\langle f \rangle = \int_{f_{ce}/20}^{f_{ce}/2} f \cdot \mathcal{E}_w^2(f)df / E_w^2$. Figure 9b shows the $\mathcal{P}(B_w, \langle f \rangle)$ distribution for the event in Figure 2, with B_w recalculated from E_w using the cold plasma dispersion (see examples in, e.g., Ni, Thorne, Meredith, Horne, & Shprits, 2011; Agapitov et al., 2014). Using this $\mathcal{P}(B_w, \langle f \rangle)$ distribution, we can rewrite the mapping Equation 1 as a two-step equation. During each half of the bounce period (time interval between two successive resonances; this is further discussed in Section 4.3), we generate a random number to select a (B_w, $\langle f \rangle$) bin from the $\mathcal{P}$ distribution. According to this number, we choose the wave amplitude B_w and wave frequency $\langle f \rangle / f_{ce}$ to calculate three main characteristics of wave-particle interactions: $\Delta\gamma_{trap}$, $\Delta\gamma_{scat}$, and π. Then, we make one iteration for energy and pitch-angle using Equation 1. Thus, the observed distribution of wave

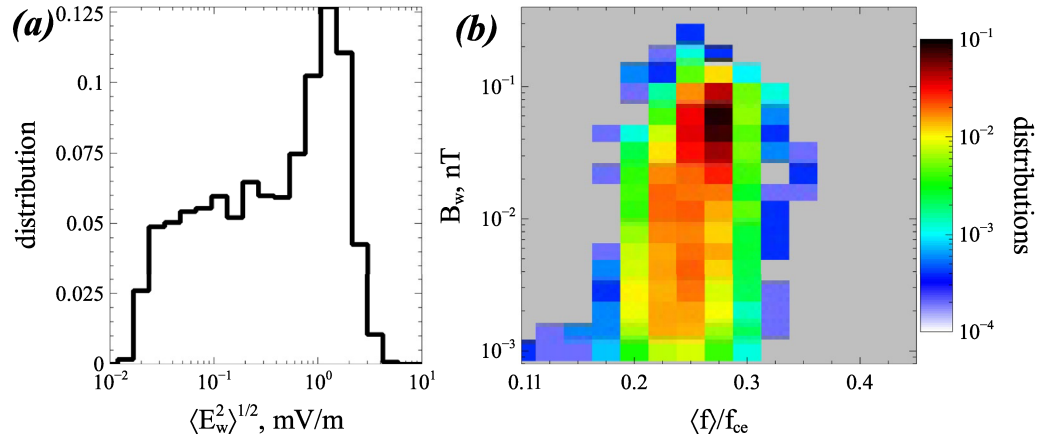

Figure 9. Panel (a) shows the distribution of electric field amplitudes derived from the wave frequency spectra (*fff* data) shown in Figure 2c. Panel (b) shows the distribution of wave amplitudes and frequencies for the event in Figure 2. Wave magnetic field amplitudes are converted from the wave electric field amplitudes using cold plasma dispersion relation (Tao & Bortnik, 2010).

characteristics, $\mathcal{P}(B_w, \langle f \rangle)$, determines $\Delta\gamma_{trap}$, $\Delta\gamma_{scat}$, and π for each resonant interaction. Figure 8c shows several examples of electron trajectories calculated with the observed $\mathcal{P}$ distribution.

3.2. Simulation Results

Using the mapping technique with the observed distribution $\mathcal{P}(B_w, \langle f \rangle)$, we integrate a large ensemble of electron trajectories having an initial (energy, pitch-angle) distribution from Figure 4. As we are interested in precipitation patterns, we restrict the integration time to ~1 bounce period of 100 keV electrons.

All electrons with $\alpha_{eq} < 2°$ are considered to be precipitating (as appropriate at $L < 8$). Figure 10a shows several pitch-angle distributions for different energies after wave-particle resonant interactions. There is a clear peak of small α_{eq} electron fluxes, and this peak is most pronounced for energies higher than ~30 keV. The formation of such a field-aligned (and partially precipitating) electron population is produced by the electron trapping acceleration in the Landau resonance. Despite the small probability of electron Landau trapping π (see, e.g., Artemyev, Krasnoselskikh, et al., 2012; Artemyev, Vasiliev, Mourenas, Agapitov, & Krasnoselskikh, 2014), this

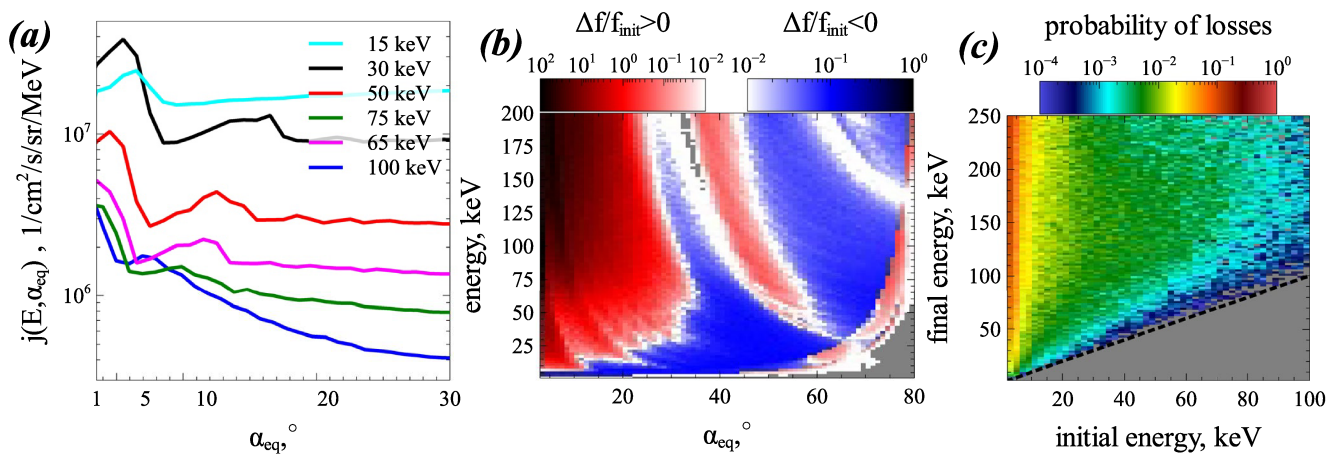

Figure 10. Results of the mapping simulation of electron nonlinear resonant interactions for the distribution of wave amplitudes and frequencies during the event in Figure 2. Panel (a) shows pitch-angle distributions for different energies after ~10 R/c ~ 2s of interactions (sufficient to make at least one bounce period for all considered particles). The initial (equatorial) electron phase space density is obtained by fitting THEMIS E observations. Panel (b) shows the ratio of final (after ~10 R/c ~ 2s) to initial phase space densities. Panel (c) shows the probability of losses, that is, the percentage of particles in each bin that is transported into the loss cone within the simulation interval (~10 R/c ~ 2s). We use a $K = 3$ factor for this simulation, with the corresponding probability of wave-particle interactions $1/K^2$.

acceleration mechanism is quite effective, because waves trap particles with initially smaller energies (~ a few keV) and accelerate them up to ~30–100 keV. Therefore, the large difference of initial phase space densities in the energy of trapping and release compensates the small probability of such trapping (π) and allows for the formation of a very substantial field-aligned electron population. Figure 10b shows the ratio of final (after the wave-particle interaction) to initial phase space densities: there is a clear particle transport toward the domain of smaller pitch-angles and larger energies. An additional effect of Landau trapping acceleration is a flux enhancement at intermediate (medium to high) pitch-angles that can produce a butterfly distribution (see also Ke et al., 2022; Mourenas et al., 2016).

The time-scale of such electron acceleration and precipitation is about a bounce period, that is, the time-scale of electron transport in the Landau trapping. This represents an insufficiently long time for nonlinear wave-particle interactions to establish a fine balance between trapping and phase bunching (nonlinear scattering) and, thus, electron transport toward the loss cone (due to trapping) may not be fully compensated by electron transport to higher pitch-angles (due to bunching). After a sufficiently long wave-particle interaction, such a fine balance will establish a new distribution function without strong gradients along the resonance curve $I_x = const$ (Artemyev et al., 2019). Thus, electron precipitation associated with the Landau trapping acceleration should be provided by bursts of very oblique whistler-mode waves, and they can share properties of microbursts. To demonstrate that such precipitation events do not decrease the ~100 keV flux population, we plot the probability of electron transport into the loss cone and the final electron energy within the loss cone as a function of initial electron energy. Figure 10c shows 2D initial, final energy space, where each bin shows the percentage of particles within the loss cone with fixed initial and final energies, showing for instance that if electrons with initial energy ~10 keV are accelerated to ~100 keV, about 5% (yellow color of the color bar) of them appear in the loss cone. Figure 10c shows that precipitating electrons (within the loss cone) with a final energy of ~100 keV had very rarely an initial energy of >80 keV. Figure 10c further shows that such precipitating electrons with a final energy of ~100 keV mainly result from trapping, acceleration, and transport via Landau resonance of initially ~5 keV electrons (more than 20% of such electrons are transported into the loss cone), ~10 keV electrons (more than 5% of such electrons are transported into the loss cone), and ~20 keV electrons (more than 1% of such electrons are transported into the loss cone). However, this also demonstrates that most (>80%) of these trapped electrons actually do not precipitate, but are released from trapping at small pitch-angles outside the loss cone (see Figure 10b). Therefore, intense (microburst) precipitation events can indicate an effective electron acceleration and an increase of ~50–200 keV electron fluxes at small pitch-angles, rather than being a signal of electron flux depletion. The accelerated electrons ending up outside the loss cone, however, have already small pitch-angles, and can be later scattered into the loss cone by much weaker field-aligned whistler-mode waves (see discussions of such double-resonance mechanism of electron losses due to Landau trapping and cyclotron scattering in Mourenas et al., 2016; Ma, Mourenas, et al., 2016; Hsieh et al., 2021).

4. Discussion

In this section, we discuss the implications of sub-relativistic electron precipitation driven by nonlinear Landau trapping due to very oblique whistler-mode waves. We compare this proposed microburst precipitation mechanism with the more commonly discussed precipitation mechanism, nonlinear cyclotron resonance scattering of electrons by field-aligned whistler-mode waves (e.g., Breneman et al., 2017; L. Chen et al., 2020). We also discuss possible limitations of the proposed mechanism of nonlinear Landau trapping.

4.1. Landau Trapping Versus Cyclotron Phase Bunching

In this study, we examined the Landau resonance of ~1–100 keV electrons and very oblique whistler-mode waves. Trapping into Landau resonance results in electron acceleration and pitch-angle decrease, that is, electrons are transported by the waves to the loss cone. The alternative, and more widely investigated, mechanism of electron precipitation by intense whistler-mode waves is phase bunching due to cyclotron resonance (Bell, 1984; Karpman et al., 1974; Karpman & Shkliar, 1977). In contrast to Landau trapping, cyclotron phase bunching is associated with an electron energy decrease (e.g., Albert, 2000), so that precipitating electrons provide whistler-wave amplification (e.g., Demekhov, Taubenschuss, & Santolík, 2017; Omura, 2021; Shklyar, 2017; Tao et al., 2021). There are two questions that merit further discussion at this point: (a) can we distinguish precipitation due to Landau

trapping from that which is due to cyclotron scattering? (b) would cyclotron scattering result in a depletion of radiation belt energetic electron fluxes, contrary to Landau trapping which do not deplete such fluxes?

To address the first question, we analyze resonant energies for both Landau trapping and cyclotron phase bunching. For monochromatic waves, the resonant wave-particle interaction conserves the invariant $m_e c^2 n_r \gamma - I_x \omega$, with $n_r = 0$ for the Landau resonance and $n_r = 1$ for the cyclotron resonance (e.g., Shklyar & Matsumoto, 2009). These invariants define resonance curves in the energy and pitch-angle space, and resonant interaction moves particles along these curves (Summers et al., 1998). Figure 1 shows the resonance curves for cyclotron and Landau resonance: Landau trapping results in a significant energy increase and transport into the loss cone, whereas cyclotron bunching near the loss cone does not change the electron energy significantly. Therefore, we examine resonant energies in the case of cyclotron bunching and energies at the time of release from resonance in the case of Landau trapping. We first consider the 2D parametric space of wave frequency, $\omega/\Omega_{ce,eq}$, and latitude of precipitation, λ_R (latitude where electrons are moved into the loss cone). This is the latitude of cyclotron resonance for phase bunching, or the latitude of electron release from Landau trapping. Figures 11a and 11b shows precipitating resonant electron energies in ($\omega/\Omega_{ce,eq}$, λ_R) space for cyclotron bunching by field-aligned waves (yellow curves) and for Landau trapping by very oblique waves (black curves). We show the results for two values of $\omega_{pe}/\Omega_{ce,eq}$, corresponding to the typical plasma density at $L \sim 6$ with $\omega_{pe}/\Omega_{ce,eq} = 6$ (Sheeley et al., 2001), and to rarefied plasma conditions $\omega_{pe}/\Omega_{ce,eq} = 1.5$. Figures 11a and 11b) shows that for realistic latitudes $\lambda_R < 40°$ (see the wave intensity distribution with latitude in Agapitov et al., 2018), the Landau trapping would be effective only for low plasma density and can provide rapid electron precipitation at < 200 keV, whereas relativistic electron precipitation should be attributed to the cyclotron scattering at $\lambda_R \gtrsim 30°$. Therefore, if waves are confined around the equator (i.e., $\lambda_R < 20°$, as is typical for intense nightside whistler-mode waves; see Meredith et al. (2012); Agapitov et al. (2013)), only cyclotron bunching can provide <200 keV microbursts. Moreover the energy ranges and, possibly, the *MLT* ranges of microbursts, could be used to separate the two precipitation mechanisms: Landau trapping and cyclotron bunching.

To further investigate the *MLT* dependence, Figures 11c and 11d displays electron precipitating (resonant) energies in the (MLT,λ_R) space for cyclotron bunching by field-aligned waves (yellow curves) and for Landau trapping by very oblique waves (black curves) at $L = 6$. Precipitating electron energies are now calculated using empirical models (Agapitov et al., 2018) for the latitudinal variation of the power-weighted mean frequency $\omega/\Omega_{ce,eq} = \max(0.17, 0.41 - 0.012 \cdot \lambda)$ of very oblique lower-band chorus waves and of the power-weighted mean frequency $\omega/\Omega_{ce,eq} = \max(0.1, 0.35 - 0.0125 \cdot \lambda)$ of quasi-parallel chorus waves (see also Bunch et al., 2013), along with an empirical model of the equatorial plasma trough density (Sheeley et al., 2001), and an empirical model of the plasma density latitudinal variation (Denton et al., 2006). In Figures 11c and 11d, the dark green region shows the (MLT,λ_R) domain where very oblique waves have significant occurrence rates (sometimes even higher than for parallel waves) in statistics near $L = 6$, which mostly occurs during moderately disturbed periods with $Kp < 3$ or $AL > -200$ nT (Agapitov et al., 2018; Li, Santolik, et al., 2016). Light green regions correspond to the (MLT,λ_R) domains of prevailing quasi-parallel chorus waves of average amplitudes >20 pT at $L = 6$, which occurs during strongly disturbed periods with $Kp > 3$ or $AL < -350$ nT (Agapitov et al., 2018). Figure 11c shows that low energy (<25 keV) microbursts due to Landau resonant interactions with very oblique waves should mainly occur at 21-13 MLT during moderately disturbed periods (with $Kp < 3$ or $AL > -200$ nT) with typical plasma trough density levels (with $\omega_{pe}/\Omega_{ce,eq} \sim 6$). In contrast, cyclotron resonance with parallel waves should lead to microbursts of much higher energies, up to ~150–250 keV at 4–12 MLT, more frequent during strongly disturbed periods (with $Kp > 3$ or $AL < -350$ nT).

However, Figure 11d also indicates that Landau resonant interactions with very oblique waves can produce microbursts of higher energies at $L = 6$, extending up to ~100–150 keV at 21-13 MLT during moderately disturbed periods (with $Kp < 3$ or $AL > -200$ nT) of strongly reduced plasma density, such that $\omega_{pe}/\Omega_{ce,eq} \sim 2$. These unusual conditions (Sheeley et al., 2001) can be encountered in the aftermath of a strong solar wind dynamic pressure pulse, as for the 2021-01-01 event in Figures 2–7 which took place 11 days after a peak of the solar wind dynamic pressure at 13.9 nPa (similar peaks preceding the events have been shown in Zhang, Artemyev, et al., 2022). For such a low plasma density, cyclotron resonance with parallel waves could easily produce 1.0–1.5-MeV microbursts, more frequent during $Kp > 3$ periods. The results in Figure 11 therefore help to distinguish microbursts driven by very oblique or parallel whistler-mode waves. In addition, Figures 11c and 11d shows that a lower plasma trough density in the 21-08 MLT sector (Sheeley et al., 2001), combined with the higher occurrences of

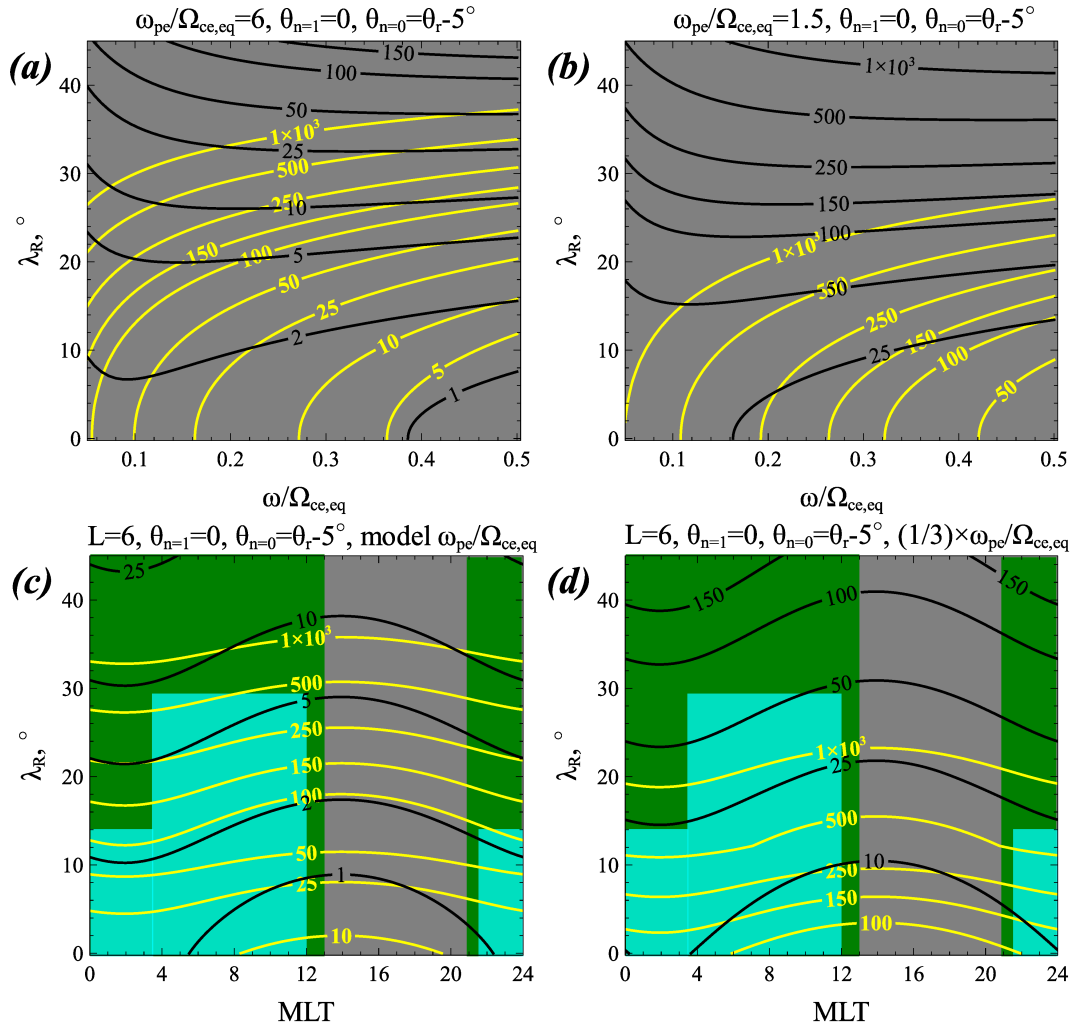

Figure 11. (a, b) Energy of precipitating electrons as a function of resonant latitude and wave frequency, for Landau resonance (black) with very oblique waves ($\theta = \theta_r - 5°$) and for cyclotron resonance (yellow) with field-aligned waves ($\theta = 0°$) at $L = 6$, for $\omega_{pe}/\Omega_{ce,eq} = 6$ (a) or 1.5 (b) and fixed ω. (c) Same as (a) at $L = 6$, but as a function of *MLT* and latitude of resonance, using empirical models of the latitudinal variation of the typical observed frequency of very oblique or parallel lower-band chorus waves (Agapitov et al., 2018) and empirical models of plasma trough density (Denton et al., 2006; Sheeley et al., 2001). Dark green colors show domains of significant occurrence of very oblique waves at $L = 6$ (as shown by previous statistics) during moderately disturbed periods with $Kp < 3$ or $AL > -200$ nT (Agapitov et al., 2018; Li, Santolik, et al., 2016). Light green color indicates regions of prevailing quasi-parallel chorus waves of average amplitudes >20 pT (as shown by previous statistics) during strongly disturbed periods with $Kp > 3$ or $AL < -350$ nT (Agapitov et al., 2018; Li, Santolik, et al., 2016). (d) Same as (c) but with a reduction (by a factor 1/3) of the model $\omega_{pe}/\Omega_{ce,eq}$.

very oblique waves and the presence of parallel waves at higher latitudes in the 04–12 MLT sector (Agapitov et al., 2018; Li, Santolik, et al., 2016), should lead to higher-energy microbursts in the 04–08 MLT sector for both mechanisms.

To address the second question, let us examine in detail the electron nonlinear resonant interaction with field-aligned whistler-mode waves. This interaction combines phase bunching (energy and pitch-angle decrease) and phase trapping (energy and pitch-angle increase) (e.g., Shklyar & Matsumoto, 2009). Trapping and bunching are in a fine balance that ultimately flattens the initial phase space density gradients along the resonance curves, $m_e c^2 \gamma - I_x \omega = const$ (e.g., Artemyev et al., 2019; Artemyev, Neishtadt, et al., 2016). Electron precipitation due to phase bunching is accompanied by acceleration of other electrons that experience phase trapping. The cyclotron phase trapping can provide an electron energy increase up to hundreds of keV, even up to a few MeVs at $\alpha_{eq} > 60°$ (e.g., Hsieh et al., 2020; Hsieh & Omura, 2017a; Omura et al., 2007). Therefore, microbursts driven

by Landau trapping should be associated with the formation of an accelerated field-aligned (<200 keV) electron population, whereas microbursts driven by cyclotron bunching should be associated with the formation of a transversely accelerated (up to MeVs) electron population. Accordingly, the actual contribution of microbursts to the depletion of the outer radiation belt ought to be investigated through detailed comparisons of simulations with observed electron flux dynamics (in different energy and pitch-angle domains) in response to nonlinear resonant interactions.

4.2. On the Importance of Wave Coherence

All existing theoretical models of electron nonlinear resonant interactions with whistler-mode waves operate with highly coherent monochromatic ($\partial\omega/\partial t = 0$) or weakly non-monochromatic (i.e., with $\partial\omega/\partial t \neq 0$, but $\partial\omega/\partial t \ll \omega^2$) waves (see, e.g., Demekhov et al., 2006; Shklyar & Matsumoto, 2009; Albert et al., 2013; Omura et al., 2015; Artemyev, Neishtadt, Vainchtein, et al., 2018, and references therein). However, numerical simulations (see Zhang et al., 2021; Mourenas et al., 2022, and references therein) and spacecraft observations (e.g., Zhang, Mourenas, et al., 2020; Zhang, Agapitov, et al., 2020, and references therein) show that intense whistler-mode waves often propagate in weakly coherent, short wave-packets, with only ∼5–10 wave periods within a packet. Such a strong wave amplitude modulation is typical for both quasi-parallel (e.g., Santolík, Kletzing, et al., 2014; Tsurutani et al., 2011; Tsurutani et al., 2020) and very oblique (e.g., Agapitov et al., 2014) waves. Loss of coherence and strong wavefield modulation are critically important for the nonlinear resonant interaction, because these effects destroy long-term resonances and limit trapping acceleration (Allanson et al., 2021; An et al., 2022; Artemyev, Mourenas, et al., 2015; Brinca, 1972; Gan et al., 2022; Tao et al., 2013). Therefore, an accurate quantification of nonlinear resonant interactions for electron precipitation via Landau trapping requires a further generalization of theoretical models for weakly coherent waves.

4.3. On the Resonance Overlapping

In our mapping simulation, we set the time interval between two successive resonant interactions as one half of the bounce period, that is, we assume that there is only one resonance during this interval. This assumption is supported by observations of intense whistler-mode wave packets that often propagate at some distance from each other, each packet occupying a sufficient fraction of the magnetic field line to exclude the possibility of electrons reaching resonance with two similar wave packets within a half bounce period (see discussions in, e.g., Artemyev, Krasnoselskikh, et al., 2012; Zhang et al., 2018). However, this does not exclude the possibility of multiple resonances (attaining $|n_r| \gg 1$) with the same wave-packet (e.g., Artemyev, Agapitov, et al., 2012; Shklyar, 1981; Shklyar, 2009). The effects from each of these cyclotron resonances can sometimes be comparable (e.g., Artemyev, Mourenas, et al., 2013; Mourenas et al., 2012). For weakly oblique whistler-mode waves, the contribution of high-order cyclotron resonances to electron diffusion is quite low (e.g., Shprits & Ni, 2009), but diffusion by very oblique whistler-mode waves can become very effective if these waves are not purely electrostatic (see discussions in Artemyev, Agapitov, et al., 2016; Li et al., 2014; Mourenas et al., 2014; Albert, 2017). Therefore, the inclusion of higher-order resonance effects into the mapping model of electron resonances with whistler-mode waves can potentially alter the rates of electron precipitation and acceleration via nonlinear Landau trapping (see discussions in Nunn & Omura, 2015; Hsieh & Omura, 2017a). For typical plasma and magnetic field conditions, these higher-order resonances do not overlap (Solovev & Shkliar, 1986) and can be considered separately, without destruction of the nonlinear Landau trapping acceleration. The resonance overlapping, the most destructive effect for nonlinear wave-particle interaction, may appear only for a sufficiently broad wave spectrum, where simultaneous waves with different frequencies would destroy long-term resonances with electrons (e.g., Karpman, 1974; Shapiro & Sagdeev, 1997). For electron interaction with whistler-mode waves, such resonance overlapping significantly reduces the efficiency of the trapped electron acceleration (Allanson et al., 2020; An et al., 2022; Gan et al., 2022; Tao et al., 2013; Zhang, Agapitov, et al., 2020). Therefore, efficient and short-lived microburst electron precipitation events should probably be attributed to electron resonant interactions with highly coherent, narrow band whistler-mode waves.

4.4. On Importance of Wave Propagation Properties

The proposed model of Landau trapping acceleration is based on the assumption that very oblique whistler-mode waves can reach middle latitudes despite their obliqueness. This assumption is based on spacecraft statistics of very oblique whistler-mode wave, which indeed demonstrate the presence of these very oblique waves at middle to high latitudes (see Agapitov et al., 2012; Agapitov et al., 2013). Nevertheless, this point requires an additional discussion. The general understanding of whistler-mode wave generation at the equator and propagating along magnetic field lines suggests that only ducted field-aligned propagating waves may reach middle latitudes (e.g., Pasmanik & Trakhtengerts, 2005; Streltsov et al., 2012; Demekhov, Manninen, et al., 2017; Pasmanik & Demekhov, 2020; Ke et al., 2021; R. Chen, Gao, Lu, Chen, et al., 2021), whereas the wave normal angle of non-ducted waves rapidly increases during their propagation to higher latitudes, leading to significant deviation from the source region's magnetic field lines and strong damping of the waves before they reach middle/high latitudes (e.g., Breuillard et al., 2013; L. Chen et al., 2013; Watt et al., 2013; L. Chen et al., 2021). These simulation results, however, were obtained for waves generated with small wave normal angles at the equator. In contrast, our wave model is based on a different population of waves, observed with very oblique wave normal angles already near their equatorial source region in the presence of a reduced Landau damping due to a small plateau/beam electron population (e.g., Agapitov et al., 2016; Li, Mourenas, et al., 2016; Mourenas et al., 2015). Such very oblique waves can propagate with little attenuation up to middle/high latitudes due to their reduced Landau damping (Agapitov et al., 2013, 2018; Ma et al., 2017), and they may also propagate guided inside field-aligned ducts or micro-ducts with appropriate parameters (Streltsov et al., 2006; Streltsov & Goyal, 2021; R. Chen, Gao, Lu, Tsurutani, & Wang, 2021). Nevertheless, further investigations of the spatial scales occupied by these very oblique waves, their cross-field coherence scale, and its evolution with wave propagation (see discussion in Tsurutani et al., 2011) are required to estimate the related possible constraints on electron acceleration through Landau trapping due to cross-field motion and decoherence of very oblique waves at middle latitudes.

5. Conclusions

In this study, we investigated intense sub-relativistic electron precipitation (microbursts) observed by low-altitude ELFIN spacecraft in conjunction with equatorial THEMIS E spacecraft observations of very oblique whistler-mode (lower-band) chorus waves. Combining ELFIN and THEMIS E measurements with DMSP observations, and the theoretical model of electron resonant interaction with very-oblique whistler-mode waves, we have drawn the following conclusions:

1. Intense, short-lived precipitation of $\lesssim$200 keV electrons can be produced by electron nonlinear Landau resonance with very oblique whistler-mode waves. The associated Landau resonant trapping results in electron acceleration and transport into the loss cone: electrons with initial energies of a few keV are trapped into the Landau resonance and accelerated up to $\lesssim$200 keV.
2. Such precipitation of $\lesssim$200 keV particles cannot deplete trapped electron fluxes at the same energy, but rather indicate an enhancement of the trapped $\lesssim$200 keV electron population at small pitch-angles.
3. Sub-relativistic ($\lesssim$200 keV) precipitation events observed on low-altitude spacecraft are a good indicator of such near-equatorial electron acceleration through Landau trapping by very oblique waves.
4. Sub-relativistic ($\lesssim$200 keV) electron precipitation through Landau trapping by very oblique waves requires low plasma trough densities during moderately disturbed periods (e.g., in the aftermath of a solar wind dynamic pressure pulse), and could lead to higher precipitating electron energies at 04–08 MLT. In contrast, relativistic ($\sim$500 keV) electron precipitation through cyclotron bunching by parallel waves can occur for both low and average plasma trough densities.
5. The maximum energy of precipitating electrons is roughly 10 times smaller for Landau trapping by very oblique waves than for cyclotron bunching by parallel waves at $L \sim 6$. Microbursts driven by Landau trapping of very oblique waves should be more frequent during weakly disturbed periods ($Kp < 3$), whereas microbursts driven by cyclotron bunching by parallel waves should be more frequent/efficient during disturbed periods ($Kp > 3$).
6. The efficiency of nonlinear Landau resonant interaction, resulting in intense (microburst) precipitation, shows that the population of very oblique whistler-mode waves may significantly alter sub-relativistic electron flux dynamics and should be included into radiation belt models.

Data Availability Statement

ELFIN data is available at https://data.elfin.ucla.edu/, THEMIS data is available at http://themis.ssl.berkeley.edu. Data analysis was done using SPEDAS V4.1 Angelopoulos et al. (2019) available at https://spedas.org/.

Acknowledgments
A.V.A., X.-J.Z., and Y.Z. acknowledge support by NASA award 80NSSC21K0729, A.V.A. and X.-J.Z. acknowledge support by NASA award 80NSSC18K1112, D.V. acknowledges support by NASA award 80NSSC19K0266, and A.V.A., X.-J.Z., and V.A. acknowledge support by NSF grants NSF-1914594, AGS-1242918, AGS-2019950, and AGS-2021749. We are grateful to NASA's CubeSat Launch Initiative for ELFIN's successful launch in the desired orbits. We acknowledge early support of ELFIN project by the AFOSR, under its University Nanosat Program, UNP-8 project, contract FA9453-12-D-0285, and by the California Space Grant program. We acknowledge critical contributions of numerous volunteer ELFIN team student members.

References

Agapitov, O. V., Artemyev, A., Krasnoselskikh, V., Khotyaintsev, Y. V., Mourenas, D., Breuillard, H., et al. (2013). Statistics of whistler mode waves in the outer radiation belt: Cluster STAFF-SA measurements. *Journal of Geophysical Research*, *118*(6), 3407–3420. https://doi.org/10.1002/jgra.50312

Agapitov, O. V., Artemyev, A., Mourenas, D., Krasnoselskikh, V., Bonnell, J., Le Contel, O., et al. (2014). The quasi-electrostatic mode of chorus waves and electron nonlinear acceleration. *Journal of Geophysical Research*, *119*(3), 1606–1626. https://doi.org/10.1002/2013JA019223

Agapitov, O. V., Artemyev, A. V., Mourenas, D., Mozer, F. S., & Krasnoselskikh, V. (2015a). Empirical model of lower band chorus wave distribution in the outer radiation belt. *Journal of Geophysical Research*, *120*(12), 10–425. https://doi.org/10.1002/2015JA021829

Agapitov, O. V., Artemyev, A. V., Mourenas, D., Mozer, F. S., & Krasnoselskikh, V. (2015b). Nonlinear local parallel acceleration of electrons through Landau trapping by oblique whistler mode waves in the outer radiation belt. *Geophysical Research Letters*, *42*(23), 10. https://doi.org/10.1002/2015GL066887

Agapitov, O. V., Krasnoselskikh, V., Khotyaintsev, Y. V., & Rolland, G. (2012). Correction to "A statistical study of the propagation characteristics of whistler waves observed by Cluster". *Geophysical Research Letters*, *39*(24), 24102. https://doi.org/10.1029/2012GL054320

Agapitov, O. V., Mourenas, D., Artemyev, A. V., & Mozer, F. S. (2016). Exclusion principle for very oblique and parallel lower band chorus waves. *Geophysical Research Letters*, *43*(21), 11112–11120. https://doi.org/10.1002/2016GL071250

Agapitov, O. V., Mourenas, D., Artemyev, A. V., Mozer, F. S., Hospodarsky, G., Bonnell, J., & Krasnoselskikh, V. (2018). Synthetic empirical chorus wave model from combined van allen probes and cluster statistics. *Journal of Geophysical Research*, *123*(1), 297–314. https://doi.org/10.1002/2017JA024843

Albert, J. M. (1993). Cyclotron resonance in an inhomogeneous magnetic field. *Physics of Fluids B*, *5*(8), 2744–2750. https://doi.org/10.1063/1.860715

Albert, J. M. (2000). Gyroresonant interactions of radiation belt particles with a monochromatic electromagnetic wave. *Journal of Geophysical Research*, *105*(A9), 21191–21209. https://doi.org/10.1029/2000JA000008

Albert, J. M. (2002). Nonlinear interaction of outer zone electrons with VLF waves. *Geophysical Research Letters*, *29*(8), 1275–116-3. https://doi.org/10.1029/2001GL013941

Albert, J. M. (2017). Quasi-linear diffusion coefficients for highly oblique whistler mode waves. *Journal of Geophysical Research*, *122*(5), 5339–5354. https://doi.org/10.1002/2017JA024124

Albert, J. M., & Bortnik, J. (2009). Nonlinear interaction of radiation belt electrons with electromagnetic ion cyclotron waves. *Geophysical Research Letters*, *36*(12), 12110. https://doi.org/10.1029/2009GL038904

Albert, J. M., Tao, X., & Bortnik, J. (2013). Aspects of nonlinear wave-particle interactions. In D. Summers, I. U. Mann, D. N. Baker, & M. Schulz (Eds.), *Dynamics of the earth's radiation belts and inner magnetosphere*. https://doi.org/10.1029/2012GM001324

Allanson, O., Thomas, E., Watt, C. E. J., & Neukirch, T. (2022). Weak turbulence and quasilinear diffusion for relativistic wave-particle interactions via a markov approach. *Frontiers in Physics*, *8*, 805699. https://doi.org/10.3389/fspas.2021.805699

Allanson, O., Watt, C. E. J., Allison, H. J., & Ratcliffe, H. (2021). Electron diffusion and advection during nonlinear interactions with whistler mode waves. *Journal of Geophysical Research*, *126*(5), e28793. https://doi.org/10.1029/2020JA028793

Allanson, O., Watt, C. E. J., Ratcliffe, H., Allison, H. J., Meredith, N. P., Bentley, S. N., et al. (2020). Particle-in-Cell experiments examine electron diffusion by whistler-mode waves: 2. Quasi-linear and nonlinear dynamics. *Journal of Geophysical Research*, *125*(7), e27949. https://doi.org/10.1029/2020JA027949

An, Z., Wu, Y., & Tao, X. (2022). Electron dynamics in a chorus wave field generated from particle-in-cell simulations. *Geophysical Research Letters*, *49*(3), e97778. https://doi.org/10.1029/2022GL097778

Angelopoulos, V. (2008). The THEMIS mission. *Space Science Reviews*, *141*(1–4), 5–34. https://doi.org/10.1007/s11214-008-9336-1

Angelopoulos, V., Cruce, P., Drozdov, A., Grimes, E. W., Hatzigeorgiu, N., King, D. A., et al. (2019). The space physics environment data analysis system (SPEDAS). *Space Science Reviews*, *215*(1), 9. https://doi.org/10.1007/s11214-018-0576-4

Angelopoulos, V., Tsai, E., Bingley, L., Shaffer, C., Turner, D. L., Runov, A., et al. (2020). The ELFIN mission. *Space Science Reviews*, *216*(5), 103. https://doi.org/10.1007/s11214-020-00721-7

Artemyev, A. V., Agapitov, O., Breuillard, H., Krasnoselskikh, V., & Rolland, G. (2012). Electron pitch-angle diffusion in radiation belts: The effects of whistler wave oblique propagation. *Geophysical Research Letters*, *39*(8), 8105. https://doi.org/10.1029/2012GL051393

Artemyev, A. V., Agapitov, O., Mourenas, D., Krasnoselskikh, V., Shastun, V., & Mozer, F. (2016). Oblique whistler-mode waves in the earth's inner magnetosphere: Energy distribution, origins, and role in radiation belt dynamics. *Space Science Reviews*, *200*(1–4), 261–355. https://doi.org/10.1007/s11214-016-0252-5

Artemyev, A. V., Agapitov, O. V., Mourenas, D., Krasnoselskikh, V. V., & Mozer, F. S. (2015). Wave energy budget analysis in the Earth's radiation belts uncovers a missing energy. *Nature Communications*, *6*(1), 8143. https://doi.org/10.1038/ncomms8143

Artemyev, A. V., Krasnoselskikh, V., Agapitov, O., Mourenas, D., & Rolland, G. (2012). Non-diffusive resonant acceleration of electrons in the radiation belts. *Physics of Plasmas*, *19*(12), 122901. https://doi.org/10.1063/1.4769726

Artemyev, A. V., & Mourenas, D. (2020). On whistler mode wave relation to electron field-aligned plateau populations. *Journal of Geophysical Research*, *125*(3), e27735. https://doi.org/10.1029/2019JA027735

Artemyev, A. V., Mourenas, D., Agapitov, O. V., & Krasnoselskikh, V. V. (2013). Parametric validations of analytical lifetime estimates for radiation belt electron diffusion by whistler waves. *Annales Geophysicae*, *31*(4), 599–624. https://doi.org/10.5194/angeo-31-599-2013

Artemyev, A. V., Mourenas, D., Agapitov, O. V., Vainchtein, D. L., Mozer, F. S., & Krasnoselskikh, V. V. (2015). Stability of relativistic electron trapping by strong whistler or electromagnetic ion cyclotron waves. *Physics of Plasmas*, *22*(8), 082901. https://doi.org/10.1063/1.4927774

Artemyev, A. V., Neishtadt, A. I., Vainchtein, D. L., Vasiliev, A. A., Vasko, I. Y., & Zelenyi, L. M. (2018). Trapping (capture) into resonance and scattering on resonance: Summary of results for space plasma systems. *Communications in Nonlinear Science and Numerical Simulation*, *65*, 111–160. https://doi.org/10.1016/j.cnsns.2018.05.004

Artemyev, A. V., Neishtadt, A. I., & Vasiliev, A. A. (2019). Kinetic equation for nonlinear wave-particle interaction: Solution properties and asymptotic dynamics. *Physica D: Nonlinear Phenomena*, *393*, 1–8. https://doi.org/10.1016/j.physd.2018.12.007

Artemyev, A. V., Neishtadt, A. I., & Vasiliev, A. A. (2020a). A map for systems with resonant trappings and scatterings. *Regular & Chaotic Dynamics*, *25*(1), 2–10. https://doi.org/10.1134/S1560354720010025

Artemyev, A. V., Neishtadt, A. I., & Vasiliev, A. A. (2020b). Mapping for nonlinear electron interaction with whistler-mode waves. *Physics of Plasmas*, *27*(4), 042902. https://doi.org/10.1063/1.5144477

Artemyev, A. V., Neishtadt, A. I., Vasiliev, A. A., & Mourenas, D. (2016). Kinetic equation for nonlinear resonant wave-particle interaction. *Physics of Plasmas*, *23*(9), 090701. https://doi.org/10.1063/1.4962526

Artemyev, A. V., Neishtadt, A. I., Vasiliev, A. A., & Mourenas, D. (2018). Long-term evolution of electron distribution function due to nonlinear resonant interaction with whistler mode waves. *Journal of Plasma Physics*, *84*(2), 905840206. https://doi.org/10.1017/S0022377818000260

Artemyev, A. V., Neishtadt, A. I., Vasiliev, A. A., & Mourenas, D. (2021). Transitional regime of electron resonant interaction with whistler-mode waves in inhomogeneous space plasma. *Physical Review E*, *104*(5), 055203. https://doi.org/10.1103/PhysRevE.104.055203

Artemyev, A. V., Neishtadt, A. I., Vasiliev, A. A., Zhang, X.-J., Mourenas, D., & Vainchtein, D. (2021). Long-term dynamics driven by resonant wave-particle interactions: From Hamiltonian resonance theory to phase space mapping. *Journal of Plasma Physics*, *87*(2), 835870201. https://doi.org/10.1017/S0022377821000246

Artemyev, A. V., Orlova, K. G., Mourenas, D., Agapitov, O. V., & Krasnoselskikh, V. V. (2013). Electron pitch-angle diffusion: Resonant scattering by waves vs. nonadiabatic effects. *Annales Geophysicae*, *31*(9), 1485–1490. https://doi.org/10.5194/angeo-31-1485-2013

Artemyev, A. V., Vasiliev, A. A., Mourenas, D., Agapitov, O., & Krasnoselskikh, V. (2013). Nonlinear electron acceleration by oblique whistler waves: Landau resonance vs. cyclotron resonance. *Physics of Plasmas*, *20*(12), 122901. https://doi.org/10.1063/1.4836595

Artemyev, A. V., Vasiliev, A. A., Mourenas, D., Agapitov, O., Krasnoselskikh, V., Boscher, D., & Rolland, G. (2014). Fast transport of resonant electrons in phase space due to nonlinear trapping by whistler waves. *Geophysical Research Letters*, *41*(16), 5727–5733. https://doi.org/10.1002/2014GL061380

Artemyev, A. V., Vasiliev, A. A., Mourenas, D., Agapitov, O. V., & Krasnoselskikh, V. V. (2014). Electron scattering and nonlinear trapping by oblique whistler waves: The critical wave intensity for nonlinear effects. *Physics of Plasmas*, *21*(10), 102903. https://doi.org/10.1063/1.4897945

Artemyev, A. V., Vasiliev, A. A., Mourenas, D., Neishtadt, A. I., Agapitov, O. V., & Krasnoselskikh, V. (2015). Probability of relativistic electron trapping by parallel and oblique whistler-mode waves in Earth's radiation belts. *Physics of Plasmas*, *22*(11), 112903. https://doi.org/10.1063/1.4935842

Auster, H. U., Glassmeier, K. H., Magnes, W., Aydogar, O., Baumjohann, W., Constantinescu, D., et al. (2008). The THEMIS fluxgate magnetometer. *Space Science Reviews*, *141*(1–4), 235–264. https://doi.org/10.1007/s11214-008-9365-9

Bell, T. F. (1984). The nonlinear gyroresonance interaction between energetic electrons and coherent VLF waves propagating at an arbitrary angle with respect to the earth's magnetic field. *Journal of Geophysical Research*, *89*(A2), 905–918. https://doi.org/10.1029/JA089iA02p00905

Blake, J. B., & O'Brien, T. P. (2016). Observations of small-scale latitudinal structure in energetic electron precipitation. *Journal of Geophysical Research*, *121*(4), 3031–3035. https://doi.org/10.1002/2015JA021815

Blum, L. W., Halford, A., Millan, R., Bonnell, J. W., Goldstein, J., Usanova, M., et al. (2015). Observations of coincident EMIC wave activity and duskside energetic electron precipitation on 18-19 January 2013. *Geophysical Research Letters*, *42*(14), 5727–5735. https://doi.org/10.1002/2015GL065245

Blum, L. W., Li, X., & Denton, M. (2015). Rapid MeV electron precipitation as observed by SAMPEX/HILT during high-speed stream-driven storms. *Journal of Geophysical Research*, *120*(5), 3783–3794. https://doi.org/10.1002/2014JA020633

Bonnell, J. W., Mozer, F. S., Delory, G. T., Hull, A. J., Ergun, R. E., Cully, C. M., et al. (2008). The electric field instrument (EFI) for THEMIS. *Space Science Reviews*, *141*(1–4), 303–341. https://doi.org/10.1007/s11214-008-9469-2

Bortnik, J., Thorne, R. M., Meredith, N. P., & Santolik, O. (2007). Ray tracing of penetrating chorus and its implications for the radiation belts. *Geophysical Research Letters*, *34*(15), L15109. https://doi.org/10.1029/2007GL030040

Breneman, A. W., Crew, A., Sample, J., Klumpar, D., Johnson, A., Agapitov, O., et al. (2017). Observations directly linking relativistic electron microbursts to whistler mode chorus: Van allen probes and FIREBIRD II. *Geophysical Research Letters*, *44*(22), 11265–11272. https://doi.org/10.1002/2017GL075001

Breuillard, H., Zaliznyak, Y., Agapitov, O., Artemyev, A., Krasnoselskikh, V., & Rolland, G. (2013). Spatial spreading of magnetospherically reflected chorus elements in the inner magnetosphere. *Annales Geophysicae*, *31*(8), 1429–1435. https://doi.org/10.5194/angeo-31-1429-2013

Brinca, A. L. (1972). On the stability of obliquely propagating whistlers. *Journal of Geophysical Research*, *77*(19), 3495–3507. https://doi.org/10.1029/JA077i019p03495

Bunch, N. L., Spasojevic, M., Shprits, Y. Y., Gu, X., & Foust, F. (2013). The spectral extent of chorus in the off-equatorial magnetosphere. *Journal of Geophysical Research*, *118*(4), 1700–1705. https://doi.org/10.1029/2012JA018182

Capannolo, L., Li, W., Ma, Q., Chen, L., Shen, X. C., Spence, H. E., et al. (2019). Direct observation of sub-relativistic electron precipitation potentially driven by EMIC waves. *Geophysical Research Letters*, *46*(22), 12711–12721. https://doi.org/10.1029/2019GL084202

Capannolo, L., Li, W., Millan, R., Smith, D., Sivadas, N., Sample, J., & Shekhar, S. (2022). Relativistic electron precipitation near midnight: Drivers, distribution, and properties. *Journal of Geophysical Research*, *127*(1), e2021JA030111. https://doi.org/10.1029/2021JA030111

Cattell, C., Wygant, J. R., Goetz, K., Kersten, K., Kellogg, P. J., von Rosenvinge, T., et al. (2008). Discovery of very large amplitude whistler-mode waves in Earth's radiation belts. *Geophysical Research Letters*, *35*(1), 1105. https://doi.org/10.1029/2007GL032009

Chen, L., Breneman, A. W., Xia, Z., & Zhang, X.-j. (2020). Modeling of bouncing electron microbursts induced by ducted chorus waves. *Geophysical Research Letters*, *47*(17), e89400. https://doi.org/10.1029/2020GL089400

Chen, L., Thorne, R. M., Li, W., & Bortnik, J. (2013). Modeling the wave normal distribution of chorus waves. *Journal of Geophysical Research*, *118*(3), 1074–1088. https://doi.org/10.1029/2012JA018343

Chen, L., Zhang, X.-J., Artemyev, A., Angelopoulos, V., Tsai, E., Wilkins, C., & Horne, R. B. (2022). Ducted chorus waves cause sub-relativistic and relativistic electron microbursts. *Geophysical Research Letters*, *49*(5), e97559. https://doi.org/10.1029/2021GL097559

Chen, L., Zhang, X.-J., Artemyev, A., Zheng, L., Xia, Z., Breneman, A. W., & Horne, R. B. (2021). Electron microbursts induced by nonducted chorus waves. *Frontiers in Astronomy and Space Sciences*, *8*, 163. https://doi.org/10.3389/fspas.2021.745927

Chen, L., Zhu, H., & Zhang, X. (2019). Wavenumber analysis of EMIC waves. *Geophysical Research Letters*, *46*(11), 5689–5697. https://doi.org/10.1029/2019GL082686

Chen, R., Gao, X., Lu, Q., Chen, L., Tsurutani, B. T., Li, W., & Wang, S. (2021). In situ observations of whistler mode chorus waves guided by density ducts. *Journal of Geophysical Research*, *126*(4), e28814. https://doi.org/10.1029/2020JA028814

Chen, R., Gao, X., Lu, Q., Tsurutani, B. T., & Wang, S. (2021). Observational evidence for whistler mode waves guided/ducted by the inner and outer edges of the plasmapause. *Geophysical Research Letters*, *48*(6), e92652. https://doi.org/10.1029/2021GL092652

Chen, R., Gao, X., Lu, Q., & Wang, S. (2019). Unraveling the correlation between chorus wave and electron beam-like distribution in the earth's magnetosphere. *Geophysical Research Letters*, *46*(21), 11671–11678. https://doi.org/10.1029/2019GL085108

Cully, C. M., Bonnell, J. W., & Ergun, R. E. (2008). THEMIS observations of long-lived regions of large-amplitude whistler waves in the inner magnetosphere. *Geophysical Research Letters*, *35*, 17. https://doi.org/10.1029/2008GL033643

Cully, C. M., Ergun, R. E., Stevens, K., Nammari, A., & Westfall, J. (2008). The THEMIS digital fields board. *Space Science Reviews*, *141*(1–4), 343–355. https://doi.org/10.1007/s11214-008-9417-1

Demekhov, A. G., Manninen, J., Santolík, O., & Titova, E. E. (2017). Conjugate ground-spacecraft observations of VLF chorus elements. *Geophysical Research Letters*, *44*(23), 11735–11744. https://doi.org/10.1002/2017GL076139

Demekhov, A. G., Taubenschuss, U., & Santolík, O. (2017). Simulation of VLF chorus emissions in the magnetosphere and comparison with THEMIS spacecraft data. *Journal of Geophysical Research*, *122*(1), 166–184. https://doi.org/10.1002/2016JA023057

Demekhov, A. G., Trakhtengerts, V. Y., Rycroft, M. J., & Nunn, D. (2006). Electron acceleration in the magnetosphere by whistler-mode waves of varying frequency. *Geomagnetism and Aeronomy*, *46*(6), 711–716. https://doi.org/10.1134/S0016793206060053

Denton, R. E., Takahashi, K., Galkin, I. A., Nsumei, P. A., Huang, X., Reinisch, B. W., et al. (2006). Distribution of density along magnetospheric field lines. *Journal of Geophysical Research*, *111*(A4), 4213. https://doi.org/10.1029/2005JA011414

Gan, L., Li, W., Ma, Q., Albert, J. M., Artemyev, A. V., & Bortnik, J. (2020). Nonlinear interactions between radiation belt electrons and chorus waves: Dependence on wave amplitude modulation. *Geophysical Research Letters*, *47*(4), e85987. https://doi.org/10.1029/2019GL085987

Gan, L., Li, W., Ma, Q., Artemyev, A. V., & Albert, J. M. (2022). Dependence of nonlinear effects on whistler-mode wave bandwidth and amplitude: A perspective from diffusion coefficients. *Journal of Geophysical Research: Space physics*, *127*(5). https://doi.org/10.1029/2021JA030063

Grach, V. S., & Demekhov, A. G. (2020). Precipitation of relativistic electrons under resonant interaction with electromagnetic ion cyclotron wave packets. *Journal of Geophysical Research*, *125*(2), e27358. https://doi.org/10.1029/2019JA027358

Grach, V. S., Demekhov, A. G., & Larchenko, A. V. (2021). Resonant interaction of relativistic electrons with realistic electromagnetic ion-cyclotron wave packets. *Earth Planets and Space*, *73*(1), 129. https://doi.org/10.1186/s40623-021-01453-w

Hardy, D. A., Schmitt, L. K., Gussenhoven, M. S., Marshall, F. J., & Yeh, H. C. (1984). *Precipitating electron and ion detectors (SSJ/4) for the block 5D/Flights 6-10 DMSP (Defense Meteorological Satellite Program) satellites: Calibration and data presentation*. Air Force Geophysics Lab Hanscom Afb Ma.

Hiraga, R., & Omura, Y. (2020). Acceleration mechanism of radiation belt electrons through interaction with multi-subpacket chorus waves. *Earth Planets and Space*, *72*(1), 21. https://doi.org/10.1186/s40623-020-1134-3

Horne, R. B., Kersten, T., Glauert, S. A., Meredith, N. P., Boscher, D., Sicard-Piet, A., et al. (2013). A new diffusion matrix for whistler mode chorus waves. *Journal of Geophysical Research*, *118*(10), 6302–6318. https://doi.org/10.1002/jgra.50594

Horne, R. B., & Thorne, R. M. (1998). Potential waves for relativistic electron scattering and stochastic acceleration during magnetic storms. *Geophysical Research Letters*, *25*(15), 3011–3014. https://doi.org/10.1029/98GL01002

Horne, R. B., & Thorne, R. M. (2003). Relativistic electron acceleration and precipitation during resonant interactions with whistler-mode chorus. *Geophysical Research Letters*, *30*(10), 100000–100001. https://doi.org/10.1029/2003GL016973

Hsieh, Y.-K., Kubota, Y., & Omura, Y. (2020). Nonlinear evolution of radiation belt electron fluxes interacting with oblique whistler mode chorus emissions. *Journal of Geophysical Research: Space Physics*(2), e2019JA027465. Retrieved from https://agupubs.onlinelibrary.wiley.com/doi/abs/10.1029/2019JA027465

Hsieh, Y.-K., & Omura, Y. (2017a). Nonlinear dynamics of electrons interacting with oblique whistler mode chorus in the magnetosphere. *Journal of Geophysical Research*, *122*(1), 675–694. https://doi.org/10.1002/2016JA023255

Hsieh, Y.-K., & Omura, Y. (2017b). Study of wave-particle interactions for whistler mode waves at oblique angles by utilizing the gyroaveraging method. *Radio Science*, *52*(10), 1268–1281. https://doi.org/10.1002/2017RS006245

Hsieh, Y.-K., Omura, Y., & Kubota, Y. (2021). Energetic electron precipitation induced by oblique whistler mode chorus emissions. *Earth and Space Science Open Archive*, *30*. https://doi.org/10.1002/essoar.10507116.1

Istomin, Y. N., Karpman, V. I., & Shklyar, D. R. (1973). Nonlinear theory of a quasimonochromatic packet of electrostatic waves in an inhomogeneous plasma. *Soviet Journal of Experimental and Theoretical Physics*, *37*, 1045.

Itin, A. P., Neishtadt, A. I., & Vasiliev, A. A. (2000). Captures into resonance and scattering on resonance in dynamics of a charged relativistic particle in magnetic field and electrostatic wave. *Physica D: Nonlinear Phenomena*, *141*(3–4), 281–296. https://doi.org/10.1016/S0167-2789(00)00039-7

Karpman, V. I. (1974). Nonlinear effects in the ELF waves propagating along the magnetic field in the magnetosphere. *Space Science Reviews*, *16*(3), 361–388. https://doi.org/10.1007/BF00171564

Karpman, V. I., Istomin, J. N., & Shklyar, D. R. (1974). Nonlinear theory of a quasi-monochromatic whistler mode packet in inhomogeneous plasma. *Plasma Physics*, *16*(8), 685–703. https://doi.org/10.1088/0032-1028/16/8/001

Karpman, V. I., & Shkliar, D. R. (1977). Particle precipitation caused by a single whistler-mode wave injected into the magnetosphere. *Planatary Space Science*, *25*(4), 395–403. https://doi.org/10.1016/0032-0633(77)90055-1

Ke, Y., Chen, L., Gao, X., Lu, Q., Wang, X., Chen, R., et al. (2021). Whistler mode waves trapped by density irregularities in the earth's magnetosphere. *Geophysical Research Letters*, *48*(7), e92305. https://doi.org/10.1029/2020GL092305

Ke, Y., Gao, X., Lu, Q., Wang, X., Chen, R., Chen, H., & Wang, S. (2022). Deformation of electron distributions due to Landau trapping by the whistler-mode wave. *Geophysical Research Letters*, *49*(3), e96428. https://doi.org/10.1029/2021GL096428

Kennel, C. F. (1966). Low-frequency whistler mode. *Physics of Fluids*, *9*(11), 2190–2202. https://doi.org/10.1063/1.1761588

Kennel, C. F. (1969). Consequences of a magnetospheric plasma. *Reviews of Geophysics and Space Physics*, *7*(1, 2), 379–419. https://doi.org/10.1029/RG007i001p00379

Kersten, T., Horne, R. B., Glauert, S. A., Meredith, N. P., Fraser, B. J., & Grew, R. S. (2014). Electron losses from the radiation belts caused by EMIC waves. *Journal of Geophysical Research*, *119*(11), 8820–8837. https://doi.org/10.1002/2014JA020366

Kong, Z., Gao, X., Chen, H., Lu, Q., Chen, R., Ke, Y., & Wang, S. (2021). The correlation between whistler mode waves and electron beam-like distribution: Test particle simulations and THEMIS observations. *Journal of Geophysical Research*, *126*(11), e29834. https://doi.org/10.1029/2021JA029834

Kubota, Y., & Omura, Y. (2017). Rapid precipitation of radiation belt electrons induced by EMIC rising tone emissions localized in longitude inside and outside the plasmapause. *Journal of Geophysical Research*, *122*(1), 293–309. https://doi.org/10.1002/2016JA023267

Kubota, Y., Omura, Y., & Summers, D. (2015). Relativistic electron precipitation induced by EMIC-triggered emissions in a dipole magnetosphere. *Journal of Geophysical Research*, *120*(6), 4384–4399. https://doi.org/10.1002/2015JA021017

Le Contel, O., Roux, A., Robert, P., Coillot, C., Bouabdellah, A., de La Porte, B., et al. (2008). First results of the THEMIS search coil magnetometers. *Space Science Reviews*, *141*(1–4), 509–534. https://doi.org/10.1007/s11214-008-9371-y

Li, W., Bortnik, J., Thorne, R. M., & Angelopoulos, V. (2011). Global distribution of wave amplitudes and wave normal angles of chorus waves using THEMIS wave observations. *Journal of Geophysical Research*, *116*(A12), 12205. https://doi.org/10.1029/2011JA017035

Li, W., Bortnik, J., Thorne, R. M., Nishimura, Y., Angelopoulos, V., & Chen, L. (2011). Modulation of whistler mode chorus waves: 2. Role of density variations. *Journal of Geophysical Research*, *116*(A6), A06206. https://doi.org/10.1029/2010JA016313

Li, W., Mourenas, D., Artemyev, A., Agapitov, O., Bortnik, J., Albert, J., et al. (2014). Evidence of stronger pitch angle scattering loss caused by oblique whistler-mode waves as compared with quasi-parallel waves. *Geophysical Research Letters*, *41*(17), 6063–6070. https://doi.org/10.1002/2014GL061260

Li, W., Mourenas, D., Artemyev, A. V., Bortnik, J., Thorne, R. M., Kletzing, C. A., et al. (2016). Unraveling the excitation mechanisms of highly oblique lower band chorus waves. *Geophysical Research Letters*, *43*(17), 8867–8875. https://doi.org/10.1002/2016GL070386

Li, W., Santolik, O., Bortnik, J., Thorne, R. M., Kletzing, C. A., Kurth, W. S., & Hospodarsky, G. B. (2016). New chorus wave properties near the equator from Van Allen Probes wave observations. *Geophysical Research Letters*, *43*(10), 4725–4735. https://doi.org/10.1002/2016GL068780

Li, W., Thorne, R. M., Bortnik, J., Nishimura, Y., & Angelopoulos, V. (2011). Modulation of whistler mode chorus waves: 1. Role of compressional pc4-5 pulsations. *Journal of Geophysical Research*, *116*(A6), A06205. https://doi.org/10.1029/2010JA016312

Li, W., Thorne, R. M., Nishimura, Y., Bortnik, J., Angelopoulos, V., McFadden, J. P., et al. (2010). THEMIS analysis of observed equatorial electron distributions responsible for the chorus excitation. *Journal of Geophysical Research*, *115*(A6). https://doi.org/10.1029/2009JA014845

Ma, Q., Artemyev, A. V., Mourenas, D., Li, W., Thorne, R. M., Kletzing, C. A., et al. (2017). Very oblique whistler mode propagation in the radiation belts: Effects of hot plasma and Landau damping. *Geophysical Research Letters*, *44*(24), 12057–12066. https://doi.org/10.1002/2017GL075892

Ma, Q., Li, W., Bortnik, J., Thorne, R. M., Chu, X., Ozeke, L. G., et al. (2018). Quantitative evaluation of radial diffusion and local acceleration processes during GEM challenge events. *Journal of Geophysical Research*, *123*(3), 1938–1952. https://doi.org/10.1002/2017JA025114

Ma, Q., Li, W., Thorne, R. M., Bortnik, J., Reeves, G. D., Kletzing, C. A., et al. (2016). Characteristic energy range of electron scattering due to plasmaspheric hiss. *Journal of Geophysical Research*, *121*(12), 11. https://doi.org/10.1002/2016JA023311

Ma, Q., Li, W., Thorne, R. M., Nishimura, Y., Zhang, X.-J., Reeves, G. D., et al. (2016). Simulation of energy-dependent electron diffusion processes in the Earth's outer radiation belt. *Journal of Geophysical Research*, *121*(5), 4217–4231. https://doi.org/10.1002/2016JA022507

Ma, Q., Mourenas, D., Artemyev, A., Li, W., Thorne, R. M., & Bortnik, J. (2016). Strong enhancement of 10–100 keV electron fluxes by combined effects of chorus waves and time domain structures. *Geophysical Research Letters*, *43*(10), 4683–4690. https://doi.org/10.1002/2016GL069125

Meredith, N. P., Horne, R. B., & Anderson, R. R. (2001). Substorm dependence of chorus amplitudes: Implications for the acceleration of electrons to relativistic energies. *Journal of Geophysical Research*, *106*(A7), 13165–13178. https://doi.org/10.1029/2000JA900156

Meredith, N. P., Horne, R. B., Sicard-Piet, A., Boscher, D., Yearby, K. H., Li, W., & Thorne, R. M. (2012). Global model of lower band and upper band chorus from multiple satellite observations. *Journal of Geophysical Research*, *117*(A10), 10225. https://doi.org/10.1029/2012JA017978

Millan, R. M., & Thorne, R. M. (2007). Review of radiation belt relativistic electron losses. *Journal of Atmospheric and Solar-Terrestrial Physics*, *69*(3), 362–377. https://doi.org/10.1016/j.jastp.2006.06.019

Min, K., & Liu, K. (2016). Proton velocity ring-driven instabilities in the inner magnetosphere: Linear theory and particle-in-cell simulations. *Journal of Geophysical Research*, *121*(1), 475–491. https://doi.org/10.1002/2015JA022042

Mithaiwala, M., Crabtree, C., Ganguli, G., Rudakov, L., & Keika, K. (2013). Convective amplification of electromagnetic ion cyclotron waves from ring-distribution protons in the inner magnetosphere. *Journal of Geophysical Research*, *118*(12), 7538–7544. https://doi.org/10.1002/2013JA019134

Miyoshi, K. Y., Hosokawa, S., Kurita, S.-I., Oyama, Y., Ogawa, S., Saito, I., et al. (2021). Penetration of MeV electrons into the mesosphere accompanying pulsating aurorae. *Scientific Reports*, *11*(1), 13724. https://doi.org/10.1038/s41598-021-92611-3

Miyoshi, Y., Saito, S., Kurita, S., Asamura, K., Hosokawa, K., Sakanoi, T., et al. (2020). Relativistic electron microbursts as high-energy tail of pulsating aurora electrons. *Geophysical Research Letters*, *47*(21), e90360. https://doi.org/10.1029/2020GL090360

Mourenas, D., Artemyev, A. V., Agapitov, O. V., & Krasnoselskikh, V. (2014). Consequences of geomagnetic activity on energization and loss of radiation belt electrons by oblique chorus waves. *Journal of Geophysical Research*, *119*(4), 2775–2796. https://doi.org/10.1002/2013JA019674

Mourenas, D., Artemyev, A. V., Agapitov, O. V., Krasnoselskikh, V., & Mozer, F. S. (2015). Very oblique whistler generation by low-energy electron streams. *Journal of Geophysical Research*, *120*(5), 3665–3683. https://doi.org/10.1002/2015JA021135

Mourenas, D., Artemyev, A. V., Agapitov, O. V., Mozer, F. S., & Krasnoselskikh, V. V. (2016). Equatorial electron loss by double resonance with oblique and parallel intense chorus waves. *Journal of Geophysical Research*, *121*(5), 4498–4517. https://doi.org/10.1002/2015JA022223

Mourenas, D., Artemyev, A. V., Ripoll, J.-F., Agapitov, O. V., & Krasnoselskikh, V. V. (2012). Timescales for electron quasi-linear diffusion by parallel and oblique lower-band Chorus waves. *Journal of Geophysical Research*, *117*(A6), A06234. https://doi.org/10.1029/2012JA017717

Mourenas, D., Ma, Q., Artemyev, A. V., & Li, W. (2017). Scaling laws for the inner structure of the radiation belts. *Geophysical Research Letters*, *44*(7), 3009–3018. https://doi.org/10.1002/2017GL072987

Mourenas, D., & Ripoll, J.-F. (2012). Analytical estimates of quasi-linear diffusion coefficients and electron lifetimes in the inner radiation belt. *Journal of Geophysical Research*, *117*(A1), A01204. https://doi.org/10.1029/2011JA016985

Mourenas, D., Zhang, X.-J., Artemyev, A. V., Angelopoulos, V., Thorne, R. M., Bortnik, J., et al. (2018). Electron nonlinear resonant interaction with short and intense parallel chorus wave packets. *Journal of Geophysical Research*, *123*(6), 4979–4999. https://doi.org/10.1029/2018JA025417

Mourenas, D., Zhang, X.-J., Nunn, D., Artemyev, A. V., Angelopoulos, V., Tsai, E., & Wilkins, C. (2022). Short chorus wave packets: Generation within chorus elements, statistics, and consequences on energetic electron precipitation. *Journal of Geophysical Research: Space Physics*, *127*(5), e2022JA030310. https://doi.org/10.1029/2022JA030310

Mozer, F. S., Agapitov, O. V., Blake, J. B., & Vasko, I. Y. (2018). Simultaneous observations of lower band chorus emissions at the equator and microburst precipitating electrons in the ionosphere. *Geophysical Research Letters*, *45*(2), 511–516. https://doi.org/10.1002/2017GL076120

Neishtadt, A. I. (1975). Passage through a separatrix in a resonance problem with a slowly-varying parameter. *Journal of Applied Mathematics and Mechanics*, *39*(4), 594–605. https://doi.org/10.1016/0021-8928(75)90060-X

Neishtadt, A. I. (1999). On adiabatic invariance in two-frequency systems In C. Simo (Ed.), *Hamiltonian systems with three or more degrees of freedom* (Vol. 533, pp. 193–213). Kluwer Academy Publications. NATO ASI Series C. https://doi.org/10.1063/1.166236

Neishtadt, A. I., Vainchtein, D., & Vasiliev, A. (2011). Dynamics of electrons in a parabolic magnetic field perturbed by an electromagnetic wave. *Plasma Physics and Controlled Fusion*, *53*(8), 085014. https://doi.org/10.1088/0741-3335/53/8/085014

Ni, B., Cao, X., Zou, Z., Zhou, C., Gu, X., Bortnik, J., et al. (2015). Resonant scattering of outer zone relativistic electrons by multiband EMIC waves and resultant electron loss time scales. *Journal of Geophysical Research*, *120*(9), 7357–7373. https://doi.org/10.1002/2015JA021466

Ni, B., Thorne, R. M., Meredith, N. P., Horne, R. B., & Shprits, Y. Y. (2011). Resonant scattering of plasma sheet electrons leading to diffuse auroral precipitation: 2. Evaluation for whistler mode chorus waves. *Journal of Geophysical Research*, *116*(A4), 4219. https://doi.org/10.1029/2010JA016233

Ni, B., Thorne, R. M., Meredith, N. P., Shprits, Y. Y., & Horne, R. B. (2011). Diffuse auroral scattering by whistler mode chorus waves: Dependence on wave normal angle distribution. *Journal of Geophysical Research*, *116*(A10), 10207. https://doi.org/10.1029/2011JA016517

Nishimura, Y., Bortnik, J., Li, W., Thorne, R. M., Ni, B., Lyons, L. R., et al. (2013). Structures of dayside whistler-mode waves deduced from conjugate diffuse aurora. *Journal of Geophysical Research*, *118*(2), 664–673. https://doi.org/10.1029/2012JA018242

Nunn, D. (1986). A nonlinear theory of sideband stability in ducted whistler mode waves. *Planatary Space Science*, *34*(5), 429–451. https://doi.org/10.1016/0032-0633(86)90032-2

Nunn, D., & Omura, Y. (2015). A computational and theoretical investigation of nonlinear wave-particle interactions in oblique whistlers. *Journal of Geophysical Research*, *120*(4), 2890–2911. https://doi.org/10.1002/2014JA020898

Nunn, D., Zhang, X. J., Mourenas, D., & Artemyev, A. V. (2021). Generation of realistic short chorus wave packets. *Geophysical Research Letters*, *48*(7), e92178. https://doi.org/10.1029/2020GL092178

O'Brien, T. P., Looper, M. D., & Blake, J. B. (2004). Quantification of relativistic electron microburst losses during the GEM storms. *Geophysical Research Letters*, *31*(4), L04802. https://doi.org/10.1029/2003GL018621

Omura, Y. (2021). Nonlinear wave growth theory of whistler-mode chorus and hiss emissions in the magnetosphere. *Earth Planets and Space*, *73*(1), 95. https://doi.org/10.1186/s40623-021-01380-w

Omura, Y., Furuya, N., & Summers, D. (2007). Relativistic turning acceleration of resonant electrons by coherent whistler mode waves in a dipole magnetic field. *Journal of Geophysical Research*, *112*(A6), 6236. https://doi.org/10.1029/2006JA012243

Omura, Y., Katoh, Y., & Summers, D. (2008). Theory and simulation of the generation of whistler-mode chorus. *Journal of Geophysical Research*, *113*(A4), 4223. https://doi.org/10.1029/2007JA012622

Omura, Y., Miyashita, Y., Yoshikawa, M., Summers, D., Hikishima, M., Ebihara, Y., & Kubota, Y. (2015). Formation process of relativistic electron flux through interaction with chorus emissions in the Earth's inner magnetosphere. *Journal of Geophysical Research*, *120*(11), 9545–9562. https://doi.org/10.1002/2015JA021563

Osmane, A., & Lejosne, S. (2021). Radial diffusion of planetary radiation belts' particles by fluctuations with finite correlation time. *The Astrophysical Journal*, *912*(2), 142. https://doi.org/10.3847/1538-4357/abf04b

Pasmanik, D. L., & Demekhov, A. G. (2020). On the influence of propagation properties of whistler-mode waves in the Earth's magnetosphere on their cyclotron amplification. *Radiophysics and Quantum Electronics*, *63*(4), 241–256. https://doi.org/10.1007/s11141-021-10049-z

Pasmanik, D. L., & Trakhtengerts, V. Y. (2005). Dispersion properties of ducted whistlers, generated by lightning discharge. *Annales Geophysicae*, *23*(4), 1433–1439. https://doi.org/10.5194/angeo-23-1433-2005

Rich, F. J., Hardy, D. A., & Gussenhoven, M. S. (1985). Enhanced ionosphere-magnetosphere data from the DMSP satellites. *EOS Transactions*, *66*(26), 513–514. https://doi.org/10.1029/EO066i026p00513

Santolík, O., Kletzing, C. A., Kurth, W. S., Hospodarsky, G. B., & Bounds, S. R. (2014). Fine structure of large-amplitude chorus wave packets. *Geophysical Research Letters*, *41*(2), 293–299. https://doi.org/10.1002/2013GL058889

Santolík, O., Macúšová, E., Kolmašová, I., Cornilleau-Wehrlin, N., & Conchy, Y. (2014). Propagation of lower-band whistler-mode waves in the outer Van Allen belt: Systematic analysis of 11 years of multi-component data from the Cluster spacecraft. *Geophysical Research Letters*, *41*(8), 2729–2737. https://doi.org/10.1002/2014GL059815

Sazhin, S. S., & Horne, R. B. (1990). Quasilongitudinal approximation for whistler-mode waves in the magnetospheric plasma. *Planatary Space Science*, *38*(12), 1551–1553. https://doi.org/10.1016/0032-0633(90)90160-R

Sergeev, V. A., & Tsyganenko, N. A. (1982). Energetic particle losses and trapping boundaries as deduced from calculations with a realistic magnetic field model. *Planatary Space Science*, *30*(10), 999–1006. https://doi.org/10.1016/0032-0633(82)90149-0

Shapiro, V. D., & Sagdeev, R. Z. (1997). Nonlinear wave-particle interaction and conditions for the applicability of quasilinear theory. *Physics Reports*, *283*(1–4), 49–71. https://doi.org/10.1016/S0370-1573(96)00053-1

Sheeley, B. W., Moldwin, M. B., Rassoul, H. K., & Anderson, R. R. (2001). An empirical plasmasphere and trough density model: CRRES observations. *Journal of Geophysical Research*, *106*(A11), 25631–25642. https://doi.org/10.1029/2000JA000286

Shklyar, D. R. (1981). Stochastic motion of relativistic particles in the field of a monochromatic wave. *Soviet Physics Journal of Experimental and Theoretical Physics*, *53*, 1197–1192.

Shklyar, D. R. (2009). Nonlinear interaction between a resonance-mode ($k_{\|} = 0$) wave and energetic plasma particles. *Journal of Plasma Physics*, *75*(3), 319–335. https://doi.org/10.1017/S0022377808007496

Shklyar, D. R. (2011). On the nature of particle energization via resonant wave-particle interaction in the inhomogeneous magnetospheric plasma. *Annales Geophysicae*, *29*(6), 1179–1188. https://doi.org/10.5194/angeo-29-1179-2011

Shklyar, D. R. (2017). Energy transfer from lower energy to higher-energy electrons mediated by whistler waves in the radiation belts. *Journal of Geophysical Research*, *122*(1), 640–655. https://doi.org/10.1002/2016JA023263

Shklyar, D. R., & Matsumoto, H. (2009). Oblique whistler-mode waves in the inhomogeneous magnetospheric plasma: Resonant interactions with energetic charged particles. *Surveys in Geophysics*, *30*(2), 55–104. https://doi.org/10.1007/s10712-009-9061-7

Shprits, Y. Y., & Ni, B. (2009). Dependence of the quasi-linear scattering rates on the wave normal distribution of chorus waves. *Journal of Geophysical Research*, *114*(A11), 11205. https://doi.org/10.1029/2009JA014223

Shprits, Y. Y., Subbotin, D. A., Meredith, N. P., & Elkington, S. R. (2008). Review of modeling of losses and sources of relativistic electrons in the outer radiation belt II: Local acceleration and loss. *Journal of Atmospheric and Solar-Terrestrial Physics*, *70*(14), 1694–1713. https://doi.org/10.1016/j.jastp.2008.06.014

Shumko, M., Gallardo-Lacourt, B., Halford, A. J., Liang, J., Blum, L. W., Donovan, E., et al. (2021). A strong correlation between relativistic electron microbursts and patchy aurora. *Geophysical Research Letters*, *48*(18), e94696. https://doi.org/10.1029/2021GL094696

Shumko, M., Sample, J., Johnson, A., Blake, B., Crew, A., Spence, H., et al. (2018). Microburst scale size derived from multiple bounces of a microburst simultaneously observed with the FIREBIRD-II CubeSats. *Geophysical Research Letters*, *45*(17), 8811–8818. https://doi.org/10.1029/2018GL078925

Shumko, M., Turner, D. L., O'Brien, T. P., Claudepierre, S. G., Sample, J., Hartley, D. P., et al. (2018). Evidence of microbursts observed near the equatorial plane in the outer van allen radiation belt. *Geophysical Research Letters*, *45*(16), 8044–8053. https://doi.org/10.1029/2018GL078451

Solovev, V. V., & Shkliar, D. R. (1986). Particle heating by a low-amplitude wave in an inhomogeneous magnetoplasma. *Soviet Physics Journal of Experimental and Theoretical Physics*, *63*, 272–277.

Stix, T. H. (1962). *The theory of plasma waves*.

Streltsov, A. V., & Goyal, R. (2021). Whistlers in micro ducts. *Journal of Geophysical Research: Space Physics*, *126*(11), e2021JA029868. https://doi.org/10.1029/2021JA029868

Streltsov, A. V., Lampe, M., Manheimer, W., Ganguli, G., & Joyce, G. (2006). Whistler propagation in inhomogeneous plasma. *Journal of Geophysical Research*, *111*(A3), A03216. https://doi.org/10.1029/2005JA011357

Streltsov, A. V., Woodroffe, J., Gekelman, W., & Pribyl, P. (2012). Modeling the propagation of whistler-mode waves in the presence of field-aligned density irregularities. *Physics of Plasmas*, *19*(5), 052104. https://doi.org/10.1063/1.4719710

Summers, D., & Thorne, R. M. (2003). Relativistic electron pitch-angle scattering by electromagnetic ion cyclotron waves during geomagnetic storms. *Journal of Geophysical Research*, *108*(A4), 1143. https://doi.org/10.1029/2002JA009489

Summers, D., Thorne, R. M., & Xiao, F. (1998). Relativistic theory of wave-particle resonant diffusion with application to electron acceleration in the magnetosphere. *Journal of Geophysical Research*, *103*(A9), 20487–20500. https://doi.org/10.1029/98JA01740

Tao, X., & Bortnik, J. (2010). Nonlinear interactions between relativistic radiation belt electrons and oblique whistler mode waves. *Nonlinear Processes in Geophysics*, *17*(5), 599–604. https://doi.org/10.5194/npg-17-599-2010

Tao, X., Bortnik, J., Albert, J. M., Thorne, R. M., & Li, W. (2013). The importance of amplitude modulation in nonlinear interactions between electrons and large amplitude whistler waves. *Journal of Atmospheric and Solar-Terrestrial Physics*, *99*, 67–72. https://doi.org/10.1016/j.jastp.2012.05.012

Tao, X., Chan, A. A., Albert, J. M., & Miller, J. A. (2008). Stochastic modeling of multidimensional diffusion in the radiation belts. *Journal of Geophysical Research*, *113*(A7), A07212. https://doi.org/10.1029/2007JA012985

Tao, X., Zonca, F., & Chen, L. (2021). A "trap-release-amplify" model of chorus waves. *Journal of Geophysical Research: Space Physics*, *126*(9), e2021JA029585. https://doi.org/10.1029/2021JA029585

Thorne, R. M., O'Brien, T. P., Shprits, Y. Y., Summers, D., & Horne, R. B. (2005). Timescale for MeV electron microburst loss during geomagnetic storms. *Journal of Geophysical Research*, *110*(A9), 9202. https://doi.org/10.1029/2004JA010882

Tsurutani, B. T., Chen, R., Gao, X., Lu, Q., Pickett, J. S., Lakhina, G. S., et al. (2020). Lower-band "monochromatic" chorus riser subelement/wave packet observations. *Journal of Geophysical Research*, *125*(10), e28090. https://doi.org/10.1029/2020JA028090

Tsurutani, B. T., Falkowski, B. J., Verkhoglyadova, O. P., Pickett, J. S., Santolík, O., & Lakhina, G. S. (2011). Quasi-coherent chorus properties: 1. Implications for wave-particle interactions. *Journal of Geophysical Research*, *116*(A9), 9210. https://doi.org/10.1029/2010JA016237

Tsyganenko, N. A. (1989). A magnetospheric magnetic field model with a warped tail current sheet. *Planatary Space Science*, *37*(1), 5–20. https://doi.org/10.1016/0032-0633(89)90066-4

Vainchtein, D., Zhang, X. J., Artemyev, A. V., Mourenas, D., Angelopoulos, V., & Thorne, R. M. (2018). Evolution of electron distribution driven by nonlinear resonances with intense field-aligned chorus waves. *Journal of Geophysical Research*, *123*(10), 8149–8169. https://doi.org/10.1029/2018JA025654

Wang, D., & Shprits, Y. Y. (2019). On how high-latitude chorus waves tip the balance between acceleration and loss of relativistic electrons. *Geophysical Research Letters*, *46*(14), 7945–7954. https://doi.org/10.1029/2019GL082681

Watt, C. E. J., Degeling, A. W., & Rankin, R. (2013). Constructing the frequency and wave normal distribution of whistler-mode wave power. *Journal of Geophysical Research*, *118*(5), 1984–1991. https://doi.org/10.1002/jgra.50231

Williams, D. J., & Lyons, L. R. (1974). The proton ring current and its interaction with the plasmapause Storm recovery phase. *Journal of Geophysical Research*, *79*(28), 4195–4207. https://doi.org/10.1029/JA079i028p04195

Wilson, L. B., III, Cattell, C. A., Kellogg, P. J., Wygant, J. R., Goetz, K., Breneman, A., & Kersten, K. (2011). The properties of large amplitude whistler mode waves in the magnetosphere: Propagation and relationship with geomagnetic activity. *Geophysical Research Letters*, *38*(17), 17107. https://doi.org/10.1029/2011GL048671

Xia, Z., Chen, L., Dai, L., Claudepierre, S. G., Chan, A. A., Soto-Chavez, A. R., & Reeves, G. D. (2016). Modulation of chorus intensity by ULF waves deep in the inner magnetosphere. *Geophysical Research Letters*, *43*(18), 9444–9452. https://doi.org/10.1002/2016GL070280

Yahnin, A. G., Sergeev, V. A., Gvozdevsky, B. B., & Vennerstrøm, S. (1997). Magnetospheric source region of discrete auroras inferred from their relationship with isotropy boundaries of energetic particles. *Annales Geophysicae*, *15*(8), 943–958. https://doi.org/10.1007/s00585-997-0943-z

Yu, X., Yuan, Z., Wang, D., Huang, S., Qiao, Z., Yu, T., & Yao, F. (2016). Excitation of oblique O^+ band EMIC waves in the inner magnetosphere driven by hot H^+ with ring velocity distributions. *Journal of Geophysical Research*, *121*(11), 11101–11112. https://doi.org/10.1002/2016JA023221

Zhang, X. J., Agapitov, O., Artemyev, A. V., Mourenas, D., Angelopoulos, V., Kurth, W. S., et al. (2020). Phase decoherence within intense chorus wave packets constrains the efficiency of nonlinear resonant electron acceleration. *Geophysical Research Letters*, *47*(20), e89807. https://doi.org/10.1029/2020GL089807

Zhang, X.-J., Angelopoulos, V., Mourenas, D., Artemyev, A., Tsai, E., & Wilkins, C. (2022). Characteristics of electron microburst precipitation based on high-resolution elfin measurements. *Journal of Geophysical Research: Space Physics*, *127*(5), e2022JA030509. https://doi.org/10.1029/2022JA030509

Zhang, X.-J., Artemyev, A., Angelopoulos, V., Tsai, E., Wilkins, C., Kasahara, S., et al. (2022). Superfast precipitation of energetic electrons in the radiation belts of the Earth. *Nature Communications*, *13*(1), 1611. https://doi.org/10.1038/s41467-022-29291-8

Zhang, X.-J., Chen, L., Artemyev, A. V., Angelopoulos, V., & Liu, X. (2019). Periodic excitation of chorus and ECH waves modulated by ultralow frequency compressions. *Journal of Geophysical Research*, *124*(11), 8535–8550. https://doi.org/10.1029/2019JA027201

Zhang, X. J., Demekhov, A. G., Katoh, Y., Nunn, D., Tao, X., Mourenas, D., et al. (2021). Fine structure of chorus wave packets: Comparison between observations and wave generation models. *Journal of Geophysical Research*, *126*(8), e29330. https://doi.org/10.1029/2021JA029330

Zhang, X. J., Mourenas, D., Artemyev, A. V., Angelopoulos, V., Bortnik, J., Thorne, R. M., et al. (2019). Nonlinear electron interaction with intense chorus waves: Statistics of occurrence rates. *Geophysical Research Letters*, *46*(13), 7182–7190. https://doi.org/10.1029/2019GL083833

Zhang, X. J., Mourenas, D., Artemyev, A. V., Angelopoulos, V., Kurth, W. S., Kletzing, C. A., & Hospodarsky, G. B. (2020). Rapid frequency variations within intense chorus wave packets. *Geophysical Research Letters*, *47*(15), e88853. https://doi.org/10.1029/2020GL088853

Zhang, X. J., Thorne, R., Artemyev, A., Mourenas, D., Angelopoulos, V., Bortnik, J., et al. (2018). Properties of intense field-aligned lower-band chorus waves: Implications for nonlinear wave-particle interactions. *Journal of Geophysical Research*, *123*(7), 5379–5393. https://doi.org/10.1029/2018JA025390